Geochemistry Geophysics Geosystems G3

Published by AGU and the Geochemical Society

Article
Volume 14, Number 1
31 January 2013
doi:10.1029/2012GC004415
ISSN: 1525-2027

Composition of plume-influenced mid-ocean ridge lavas and glasses from the Mid-Atlantic Ridge, East Pacific Rise, Galápagos Spreading Center, and Gulf of Aden

Katherine A. Kelley, Richard Kingsley, and Jean-Guy Schilling

Graduate School of Oceanography, University of Rhode Island, Narragansett Bay Campus, Narragansett, RI, 02882 (kelley@gso.uri.edu)

[1] The global mid-ocean ridge system is peppered with localities where mantle plumes impinge on oceanic spreading centers. Here, we present new, high resolution and high precision data for 40 trace elements in 573 samples of variably plume-influenced mid-ocean ridge basalts from the Mid-Atlantic ridge, the Easter Microplate and Salas y Gomez seamounts, the Galápagos spreading center, and the Gulf of Aden, in addition to previously unpublished major element and isotopic data for these regions. Included in the data set are the unconventional trace elements Mo, Cd, Sn, Sb, W, and Tl, which are not commonly reported by most geochemical studies. We show variations in the ratios Mo/Ce, Cd/Dy, Sn/Sm, Sb/Ce, W/U, and Rb/Tl, which are expected not to fractionate significantly during melting or crystallization, as a function of proximity to plume-related features on these ridges. The Cd/Dy and Sn/Sm ratios show little variation with plume proximity, although higher Cd/Dy may signal increases in the role of garnet in the mantle source beneath some plumes. Globally, the Rb/Tl ratio closely approximates the La/Sm_N ratio, and thus provides a sensitive tracer of enriched mantle domains. The W/U ratio is not elevated at plume centers, but we find significant enrichments in W/U, and to a lesser extent the Mo/Ce and Sb/Ce ratios, at mid-ocean ridges proximal to plumes. Such enrichments may provide evidence of far-field entrainment of lower mantle material that has interacted with the core by deeply-rooted, upwelling mantle plumes.

Components: 11,800 words, 9 Figures.

Keywords: MORB; plume; spreading center; ICP-MS; trace elements.

Received 14 September 2012; **Revised** 29 November 2012; **Accepted** 16 December 2012; **Published** 31 January 2013.

Kelley K. A., R. Kingsley, and J.-G. Schilling (2013), Composition of plume-influenced mid-ocean ridge lavas and glasses from the Mid-Atlantic Ridge, East Pacific Rise, Galápagos Spreading Center, and Gulf of Aden, *Geochem. Geophys. Geosyst.*, *14*, 223–242, doi: 10.1029/2012GC004415.

1. Introduction

1.1. Hotspot-influenced Spreading Ridges

[2] Throughout the global mid-ocean ridge system, there are numerous localities where oceanic hotspots impinge upon, or otherwise influence, oceanic spreading centers. The consequences of these interactions range from elevated mantle temperatures beneath ridges, leading to increased melt production, shallower bathymetry, and thicker oceanic crust [e.g., *Klein and Langmuir*, 1987; *Sinton et al*., 2003], to unique geochemical signatures in ridge lavas, reflective of compositional variations in the mantle source [e.g., *Hanan et al*., 1986; *Schilling*, 1973; *Schilling et al*., 1976].

[3] Here, we present new high-resolution data for 40 trace elements in 573 basalts, in concert with isotope dilution analyses of parent and daughter elements for the Sr, Nd, Hf and Pb isotope systematics of these samples, and with previously-unpublished major element and isotopic data for these and other samples, from hotspot-influenced regions on four global mid-ocean ridges: The Galápagos spreading center near the Galápagos hotspot, the Easter microplate and Salas y Gomez seamount chain on the East Pacific rise, the Gulf of Aden and Asal rift approaching the Afar hotspot in Eastern Africa, and the full length of the Mid-Atlantic ridge, including regions influenced by the Iceland and Jan Mayen plumes (Reykjanes and Arctic), the Azores, the Sierra Leone plume (Equatorial), the Ascension (or Circe), St. Helena, Tristan de Cunha, Discovery and Shona anomalies, and the Bouvet triple junction. Collectively, these samples have been the subject of ~100 published papers, and although most are well-characterized for radiogenic isotope composition, few studies have reported modern, comprehensive ICP-MS data for the 40 elements we report here. The new trace element data reported here include the "unconventional" elements Mo, Cd, Sn, Sb, W and Tl, which are not routinely reported by most laboratories. The data presented here thus provide one of the first comprehensive assessments of the abundances and behaviors of these elements in mid-ocean ridge basalts, and how they may vary in hotspot mantle sources.

1.2. The MGSL Sample Repository

[4] The dredge and split samples that we report and discuss here, in addition to previously studied samples from these ridges ($n > 1300$), are permanently archived at the Marine Geological Samples Laboratory (MGSL) at the Graduate School of Oceanography, University of Rhode Island (GSO/URI). They represent one of the most extensive, systematic collections of young volcanic rocks from along the global mid-ocean ridge system. Approximately one quarter of the 70,000 km-long ridge system has been sampled and archived at MGSL, at an average interval of 40 km (Fig. 1). The MGSL facility also houses core, grab, and dredge samples from numerous marine expeditions, beyond those included in the present paper, and the full archive is searchable through the National Geophysical Data Center's database for Marine & Lacustrine Geological Samples (http://seabedsamples.org). A complete listing of the MGSL archived dredges discussed here is provided in Supplementary Table 1, and a complete listing of the individual whole-rock and glass samples is provided in Supplementary Table 2. All of these samples are openly available for scientific research, and investigators interested in requesting material for study are encouraged to review the MGSL sample distribution policy (http://www.gso.uri.edu/MGSLsite/distribution_policy.htm) and to contact the facility curator, Dr. Steven Carey (scarey@gso.uri.edu), with specific inquiries.

2. Samples

[5] The samples studied here derive from the collection efforts of 38 international marine expeditions. Here, we provide brief summaries of the expeditions and overviews of the previous work and data collected in each region. Previously published data for the samples reported in this work may be accessed through the individual references cited for each region, or through the PetDB database [http://www.petdb.org; *Lehnert et al.*, 2000].

2.1. Mid-Atlantic Ridge

[6] Samples from the Mid-Atlantic ridge (MAR) cover practically its entire length, from 78°N-55°S, with major gaps in coverage only from ~16.5°N-32.5°N and ~5°N-12°N (Fig. 1a). These samples were collected during 26 marine dredging expeditions that sampled hotspot-influenced regions of the Mid-Atlantic ridge, including the Jan Mayen, Iceland, and Azores platforms on the northern MAR, the equatorial MAR influenced by the nearby Sierra Leone plume, and the southern MAR where the ridge is influenced by the off-axis Ascension, St. Helena, Tristan de Cunha, and Discovery plumes, the apparently on-axis Shona plume, and the southern ridge termination at the Bouvet plume/triple junction. These cruises include the 2π expeditions (ABP0002 or ABP1985) of the *R/V Akademik Boris Petrov*, deployments of the *DSV Alvin* (dives 521, 525, 527, and 534; 1974), Leg AG32 of the *R/V S.A. Agulhas*, Legs A073-01 (1972) and A107-07 (1980) of the *R/V Atlantis II*, Leg AK15 of the *R/V Akademik Kurchatov* (1973), Legs CH77 (1977) and CH98 (1979) of the *R/V Jean Charcot*, Leg EW9309 of the *R/V Maurice Ewing* (1993), Legs RC1604 (1972) and RC2806 (1987) of the *R/V Robert Conrad*, Legs 25 (1978), 26 (1978), 61 (1981), and 63 (1981) of the *R/V Endeavor*, and Legs 41 (1967), 89 (1970), 100 (1971), 101 (1971), 119 (1972), 122 (1972), 123 (1972), 138 (1973), 139 (1973), and 154 (1974) of the *R/V Trident*.

[7] Previous geochemical studies of samples from these cruises report a broad spectrum of data types

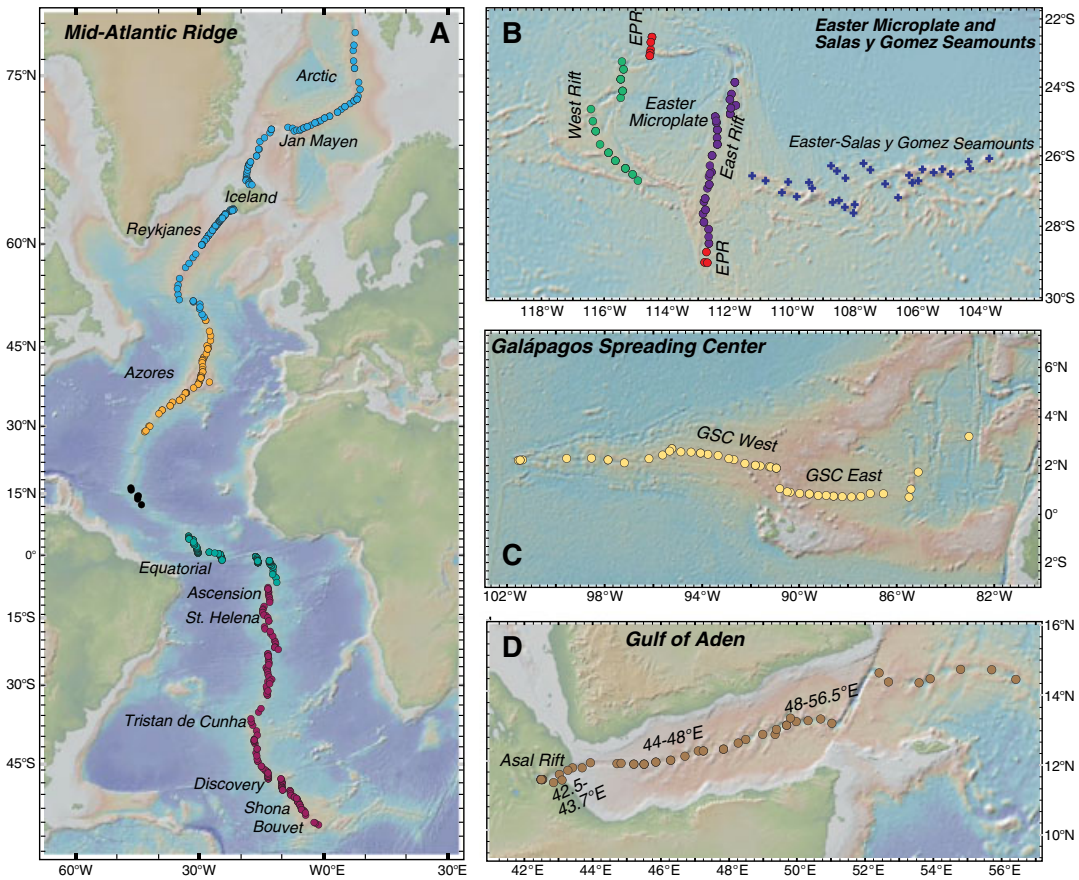

Figure 1. Regional maps showing locations of samples for which data are reported in this study. Maps were generated in GeoMapApp (http://www.geomapapp.org/) using the Global Multi-Resolution Topography synthesis base map [*Ryan et al*., 2009]. (a) The Mid-Atlantic ridge, (b) the Easter microplate and Salas y Gomez seamount chain, (c) the Galápagos spreading center, and (d) the Gulf of Aden and Asal rift.

including major elements [*Bézos and Humler*, 2005; *Bougault et al*., 1988; *Bryan and Moore*, 1977; *Christie et al*., 1986; *Dosso et al*., 1993; *Humphris et al*., 1985; *le Roex et al*., 1987; *Le Roux*, 2000; *le Roux et al*., 2002b; *Melson et al*., 2002; *Neumann and Schilling*, 1984; *Schilling*, 1973; *Schilling et al*., 1983; *Schilling et al*., 1995; *Shibata et al*., 1979; *Sigurdsson*, 1981; *van Heerden and Roex*, 1988], trace elements [*Andres et al*., 2002; *Blichert-Toft et al*., 2005; *Bougault et al*., 1988; *Bryan et al*., 1979; *Dosso et al*., 1993; *Dosso et al*., 1991; *Elkins et al*., 2011; *Hanan et al*., 2000; *Hannigan et al*., 2001; *Hémond et al*., 2006; *Humphris et al*.1985; *le Roex et al*., 1987; *Le Roux*, 2000; *le Roux et al*., 2002a; *le Roux et al*., 2002b; *Michael*, 1995; *Neumann and Schilling*, 1984; *Patchett and Tatsumoto*, 1980; *Ryan and Langmuir*, 1987; *Schiano et al*., 1997; *Schilling*, 1973; 1975; *Schilling et al*., 1999; *Schilling et al*., 1983; *Shibata et al*., 1979; *Sigurdsson and Schilling*, 1976; *Sun et al*., 1975; *van Heerden and Roex*, 1988; *Waggoner*, 1989; *White*, 1993; *White and Bryan*, 1977; *White and Schilling*, 1978; *Yu et al*., 1997], radiogenic isotopes (Sr, Nd, Pb, Hf, Os) [*Agranier et al*., 2005; *Andres et al*., 2002; 2004; *Blichert-Toft et al*., 2005; *Dosso et al*., 1993; *Dosso et al*., 1991; *Douglass et al*., 1999; *Elkins et al*., 2011; *Fontignie and Schilling*, 1996; *Hanan et al*., 1986; *Hart et al*., 1973; *Kurz et al*., 1998; *le Roex et al*., 1987; *Moore and Schilling*, 1973; *Patchett and Tatsumoto*, 1980; *Schiano et al*., 1997; *Schilling et al*., 1994; *Schilling et al*., 1999; *Sun et al*., 1975; *Waggoner*, 1989; *White*, 1979; *White and Bryan*, 1977; *White and Schilling*, 1978; *Yu et al*., 1997], dissolved volatile and halogen concentrations (H_2O, CO_2, S, Cl, F, Br) [*Dixon et al*., 2002; *Eiler et al*., 2000; *Jambon et al*., 1995; *Kingsley and Schilling*, 1995; *Michael*, 1995; *Michael and Cornell*, 1998; *Moore and Schilling*, 1973; *Pineau and Javoy*,

1994; *Rowe and Schilling*, 1979; *Schilling et al*., 1980; *Unni*, 1976; *Unni and Schilling*, 1978], light stable isotopes (δD, $\delta^{13}C$, $\delta^{18}O$) [*Eiler et al*., 2000; *Kyser and O'Neil*, 1984; *Muehlenbachs and Clayton*, 1972; *Pineau and Javoy*, 1994; *Poreda et al*., 1986], noble gas abundances and isotopes (He, Ne, Ar, Xe, Kr) [*Graham et al*., 1992; *Kurz*, 1982; *Kurz et al*., 1998; *Moreira et al*., 1995; *Poreda and Brozolo*, 1984; *Poreda et al*., 1986; *Sarda et al*., 1988; *Sarda et al*., 2000; *Schilling et al*., 1999; *Staudacher et al*., 1989], and mineral compositions [*Hermes and Schilling*, 1976; *le Roex*, 1998; *Sigurdsson and Schilling*, 1976]. Note that subsets of ICP-MS trace element data reported by *Blichert-Toft et al*. [2005] and *Hanan et al*. [2000] are duplicated here for the sake of presenting a complete data set, as these were collected at the GSO/URI ICP-MS lab using the same analytical methods and protocols as those presented here.

2.2. Easter Microplate and Salas y Gomez Seamounts

[8] Samples from the Easter microplate region of the East Pacific rise cover the main EPR spreading axes to the north and south of the microplate, and both the east and west rifts of the microplate itself, from 22°S-30°S (Fig. 1b). Dredge samples from this region were recovered by expedition PASC04WT of the *R/V Thomas Washington* (1983) and Leg 113 of the *R/V Endeavor* (1984). In addition, dredge samples from the Easter-Salas y Gomez seamount chain, which extends eastward from the Easter microplate onto the Nazca plate, extend from 112°W-103°W (Fig. 1b). The seamount chain samples were collected on expeditions YALO-74 of the *R/V Yaquina* (1973) and GLOR07MV of the *R/V Melville* (1993). This sample suite also includes three on-land samples from Easter island.

[9] Previous geochemical studies of these samples report major element concentrations [*Pan and Batiza*, 1998; *Schilling et al*., 1985], trace elements [*Fontignie and Schilling*, 1991; *Kingsley et al*., 2007; *Kingsley et al*., 2002; *Rubin and Macdougall*, 1988; 1990], dissolved volatiles and halogens (H_2O, CO_2, Cl) [*Kingsley et al*., 2002; *Simons et al*., 2002], radiogenic isotopes (Sr, Nd, Pb, Hf, U-series) [*Fontignie and Schilling*, 1991; *Hanan and Schilling*, 1989; *Kingsley and Schilling*, 1998; *Kingsley et al*., 2007; *Macdougall and Lugmair*, 1986; *Rubin and Macdougall*, 1988; 1990; *White and Hofmann*, 1982; *White et al*., 1987], and hydrogen and helium isotopes [*Kingsley et al*., 2002; *Poreda et al*., 1993]. Subsets of ICP-MS trace element data from *Kingsley et al*. [2007] and *Kingsley et al*. [2002] are duplicated here in order to provide a complete data set, as these data were collected at GSO/URI using the same analytical methods and protocols as those presented here.

2.3. Galápagos Spreading Center

[10] Samples from the Galápagos spreading center cover the main spreading axes from 83°W-102°W (Fig. 1c). These samples were collected on the SOUTHTOW expedition of the *R/V Thomas Washington* (1972-73), the COCOTOW expedition of the *R/V Melville* (1974), Leg 41 of the *R/V De Steiguer* (1974), the NAZCOPAC-17 expedition deployments of the *Nautile* submersible (1988), and Leg 164 of the *R/V Trident* (1975).

[11] Prior work on these samples has reported major elements [*Anderson et al*., 1975; *Fisk et al*., 1982; *Schilling et al*., 1976; *Schilling et al*., 1982], trace elements [*Michael*, 1988; *Schilling et al*., 2003; *Schilling et al*., 1976; *Schilling et al*., 1982; *Verma and Schilling*, 1982], radiogenic isotopes (Sr, Nd, Pb, Hf) [*Cohen and O'Nions*, 1982; *Ito et al*., 1980; *Schilling et al*., 2003; *Verma and Schilling*, 1982; *Verma et al*., 1983], CO_2 content [*Marty and Jambon*, 1987], light stable isotopes ($\delta^{13}C$, $\delta^{18}O$) [*Ito et al*., 1980; *Marty and Jambon*, 1987], noble gas abundances and isotopes (He, Ar, Ne, Xe, Kr) [*Marty and Ozima*, 1986], and phenocryst composition [*Fisk et al*., 1982]. Note that the subset of ICP-MS trace element data reported by *Schilling et al*. [2003] is duplicated here in order to provide a complete data set, as these data were collected using the same analytical methods and protocols at GSO/URI as those presented here.

2.4. Gulf of Aden and Asal Rift

[12] Samples from the Gulf of Aden cover the main spreading axes of the Sheba ridge from 43°E-57°E, extending into the Gulf of Tadjoura (Fig. 1d), and additional on-land samples extend coverage to the Asal Rift region of Africa (also know as the Ghoubbat al Kharab-Asal Rift or the Ardoukoba Rift; the extension of the Sheba Ridge over eastern Afar), from ~43°E-42.4°E. Glassy fragments from submarine cores were collected on Leg VA01 of the *R/V Valdivia* (1971; *Bäcker et al*. [1973]), and dredges were collected from Legs 33-06 and 33-07 of the *R/V Vema* (1976).

[13] The few previous studies of these samples have reported major and trace element data [*Joron*, 1980; *Schilling et al*., 1992; *Schneider and Wachendorf*,

1973] and radiogenic isotopes (Sr, Nd, Pb, Hf) [*Rooney et al*., 2012; *Schilling et al*., 1992].

3. Analytical Methods

3.1. Major Elements

3.1.1. Whole-rock

[14] Whole-rock major element data for bulk glass and lava from the Gulf of Aden and Asal Rift are reported in Supplementary Table 3. These data were collected using one of two methods, which are noted in Supplementary Table 3. Some samples were analyzed using wet chemical methods following techniques outlined by *Schilling et al*. [1983] and references therein. In summary, SiO_2, H_2O+, and H_2O- were determined by gravimetry, TiO_2 and P_2O_5 were determined by colorimetry, Al_2O_3, MgO, CaO, Na_2O, K_2O, and MnO were determined by atomic absorption spectroscopy, and FeO^T (i.e., total Fe reported as FeO) was determined by combining titration (for FeO) and difference (for Fe_2O_3) data. Other samples were analyzed for whole-rock major elements by X-ray fluorescence (XRF) spectrometry [*Cheminée*, pers. comm.].

3.1.2. Glass

[15] Glass chips were analyzed by electron microprobe in one of three laboratories. Glasses from the Mid-Atlantic ridge and the Easter Microplate/Salas y Gomez seamount chain were analyzed for major elements using the JEOL-JXA-50A electron microprobe at GSO/URI following methodologies outlined by *Schilling et al*. [1985] and *Sigurdsson* [1981]. Glass chips from the Galápagos spreading center were analyzed using either the Camebax SX50 electron microprobe at IFREMER, following methods described by *Hékinian et al*. [1995] or the ARL-EMX-SM microprobe at SUNY Stony Brook following methods outlined by *Fisk et al*. [1982]. These data are reported in Supplementary Table 4.

3.2. Radiogenic Isotopes

[16] Previously unpublished radiogenic isotope data, including $^{87}Sr/^{86}Sr$, $^{143}Nd/^{144}Nd$, $^{206}Pb/^{204}Pb$, $^{207}Pb/^{204}Pb$, $^{208}Pb/^{204}Pb$, and $^{176}Hf/^{177}Hf$, plus $^{3}He/^{4}He$ isotope ratios, for samples from the Mid-Atlantic ridge and one sample from the Easter microplate are compiled in Supplementary Table 5. These analyses were done in several laboratories, as noted in Supplementary Table 5. Some Sr-Nd-Pb isotope ratios were determined by Thermal Ionization Mass Spectrometry (TIMS) using a VG Micromass 30B single-collector, double-focusing TIMS at GSO/URI following methods outlined by *Verma and Schilling* [1982], *Verma et al*. [1983], and *Schilling et al*. [1994]. Other Sr and Nd isotope ratios were determined using a 7-collector Finnigan MAT 262 TIMS at the University of Geneva following the methods of *Fontignie and Schilling* [1991] and *Schilling et al*. [2003]. Hafnium isotope ratios were determined using the VG Plasma 54 multi-collector ICP-MS at the ENS, Lyon following methods from *Blichert-Toft et al*. [2005]. Helium isotopes were determined by mass spectrometry following methods outlined by *Poreda et al*. [1993] or *Kurz* [1982].

3.3. Trace Elements

[17] Details of trace element sample preparation and analytical methods are reported by *Kingsley* [2002], and a summary is provided here. Trace elements were determined by high-resolution inductively coupled plasma mass spectrometry (HR-ICP-MS) using both isotope dilution and external calibration methods. The isotope dilution analyses are for the parent and daughter elements that accompany the Sr, Nd, Hf and Pb isotope data of these samples, whereas the externally calibrated data encompass 40 trace elements of broad geochemical significance and utility. Sample preparation for trace element analysis was the same for both analysis methods, and spikes for either type of analysis were added to separate aliquots of the same dissolution products.

3.3.1. Sample Selection and Dissolution

[18] Glassy rims or fresh interiors were chipped from pillow lava samples, and reduced in size to <10 mm using a steel mortar. Chips were then sonicated in de-ionized H_2O, rinsed, and dried, and select chips were hand-picked under a binocular microscope to be free from visible secondary mineralization and contamination from the mortar. After picking, 100-200 mg of whole chips were weighed into PFA beakers. The chips were leached with 2N HCl for 5 minutes, then rinsed three times in triple-distilled H_2O to remove possible remaining surface contamination. Leached chips were then dissolved by adding 0.5 mL of 16N triple-distilled nitric acid and 4 mL of 29N quadruple-distilled hydrofluoric acid. Beakers were capped and heated on a hot plate at ~90°C for 24 hours before cooling and sonicating. Beakers were then opened and the contents evaporated to dryness in a HEPA-filtered drying tunnel. Dried samples were picked up in 6 mL of 8N triple-distilled nitric acid, re-capped, and heated to ~90°C

for 24 hours, followed by cooling and sonication. These final solutions were diluted to 250 mL with quadruple-distilled H_2O for analysis.

3.3.2. Isotope Dilution

[19] Abbreviated methods for isotope dilution concentration determinations are provided in *Schilling et al*. [1999]. A 5 mL aliquot of each dissolved rock solution was prepared for isotope dilution analysis by spiking with enriched isotopes of ^{230}Th, ^{235}U, ^{208}Pb, ^{147}Sm, ^{150}Nd, and ^{84}Sr using NIST Traceable standard solutions. Isotope dilution analyses used the Finnigan Element HR-ICP-MS at GSO/URI, in low resolution mode (DM/M = 300), equipped with a desolvating nebulizer. Isotope dilution analyses monitored the masses ^{230}Th, ^{232}Th, ^{235}U, ^{238}U, ^{208}Pb, ^{206}Pb, ^{147}Sm, ^{149}Sm, ^{150}Nd, ^{146}Nd, ^{84}Sr, and ^{86}Sr. At the same time, ^{87}Rb was also measured, but calibrated externally using standard solutions and monitoring drift using ^{84}Sr as an internal standard. Peak jumping and integration schemes were tuned to optimize precision on the ratios ^{230}Th/^{232}Th, ^{235}U/^{238}U, ^{208}Pb/^{206}Pb, ^{147}Sm/^{149}Sm, ^{150}Nd/^{146}Nd, and ^{84}Sr/^{86}Sr. Isotope ratios were corrected for mass bias using natural standards run at the same time. Reproducibility on 20-47 replicates of USGS and in-house standards was ≤ 3% rsd, and on average, values determined were within 1-2% difference from accepted concentrations in the standards. These data are reported in Supplementary Table 6.

3.3.3. Externally Calibrated HR-ICP-MS

[20] Methods for externally-calibrated trace element analysis were based in part on those reported by *Eggins et al*. [1997]. A 5 mL aliquot of each dissolved rock solution was spiked with Rh, In, Tm, Re, Bi as internal standards for monitoring drift. This mode of analysis also used the Finnigan Element HR-ICP-MS at GSO/URI, in low resolution mode (DM/M = 300), equipped with a desolvating nebulizer. Masses monitored for externally-calibrated trace element analyses included ^{45}Sc, ^{49}Ti, ^{51}V, ^{53}Cr, ^{59}Co, ^{60}Ni, ^{63}Cu, ^{65}Cu, ^{66}Zn, ^{67}Zn, ^{71}Ga, ^{85}Rb, ^{86}Sr, ^{88}Sr, ^{89}Y, ^{90}Zr, ^{93}Nb, ^{98}Mo, ^{114}Cd, ^{120}Sn, ^{121}Sb, ^{133}Cs, ^{137}Ba, ^{139}La, ^{140}Ce, ^{141}Pr, ^{143}Nd, ^{146}Nd, ^{147}Sm, ^{149}Sm, ^{151}Eu, ^{153}Eu, ^{157}Gd, ^{159}Tb, ^{163}Dy, ^{165}Ho, ^{167}Er, ^{172}Yb, ^{175}Lu, ^{178}Hf, ^{181}Ta, ^{184}W, ^{205}Tl, ^{206}Pb, ^{208}Pb, ^{232}Th, and ^{238}U. Instrumental drift was monitored and corrected internally using masses ^{103}Rh, ^{115}In, ^{169}Tm, ^{185}Re, and ^{209}Bi. Drift-corrected intensities were calibrated against USGS standards BCR-1, BHVO-1, BIR-1, and AGV-1, IWG standards BE-N and BR, and GSO in-house standard EN026 10D-3 (MORB from the Mohns Ridge). Preferred calibration values for these standards are provided in Supplementary Table 7. Typical calibration curves were linear ($R^2 \geq 0.999$), and replicate analyses of in-house standard EN026 10D-3 indicated overall analytical precision of <5% rsd for all elements except Sc and V, which were reproducible within 6.1% and 5.3% rsd, respectively. These trace element data are reported in Supplementary Table 8.

4. Discussion

4.1. Unconventional Trace Elements

[21] As noted above, the trace element data set reported here includes several "unconventional" trace elements that are not routinely reported in igneous geochemistry due to low natural abundances or other analytical challenges. These include siderophile transition metals Mo and W, the chalcophile/lithophile transition metal Cd, post-transition metals Sn and Tl, and the metalloid Sb. Although these elements are not as well-studied as many other trace elements, their behaviors, variations, and fractionations in igneous rocks may serve as valuable sensors of key processes in the Earth's interior.

[22] Due to their moderately siderophile behavior, Mo and W were largely segregated from the silicate Earth and partitioned into the metal phase during core formation [*Walter and Thibault*, 1995]. In the silicate mantle, however, Mo and W are highly incompatible, and thus lithophile, during mantle melting and are expected to partition similarly to Ce and U, respectively [*Arevalo and McDonough*, 2008; *Sims et al*., 1990]. The moderately chalcophile or siderophile elements Sb and Sn are also expected to partition similarly to the light REEs Ce and Sm, respectively, during mantle melting [*Jochum et al*., 1993; *Sims et al*., 1990]. Antimony and Sn may also have been preferentially extracted into the metal phase during core formation [*Righter*, 2003], and in modern settings may be mildly influenced by the presence of sulfide in the mantle or in sulfide-saturated magmas [*Jochum and Hofmann*, 1997; *Jochum et al*., 1993; *Sims et al*., 1990]. Thallium is a chalcophile element, so potentially influenced by sulfide-related processes in the mantle and in magmas, and is highly incompatible during silicate melting, expected to partition similarly to Rb [*Hertogen et al*., 1980]. Despite only weakly siderophile behavior, core formation may also have depleted the Tl concentration of the bulk silicate Earth by about 50% [*Wood et al*., 2008]. Both Sb

and Tl are also mobile in aqueous fluids and are highly enriched during alteration of submarine basaltic lavas [*Jochum and Verma*, 1996]. Cadmium is a moderately chalcophile element, and prior work has found subtle correlations between Cd and S concentrations in basaltic magmas [*Yi et al*., 2000]. In subaerial systems, Cd, like S, may partition into the volatile phase and exit magmas during degassing, although degassing is not expected to remove Cd from submarine magmas erupted at >1000 m depth [*Yi et al*., 2000]. Cadmium and Dy are expected to have similar mantle/melt partition coefficients, although the partition coefficient for the middle REE Dy may vary as a function of the presence and abundance of garnet in the mantle source [*Yi et al*., 2000].

[23] Given the expectations of similar partitioning of these elements to more conventional, lithophile trace elements, we examine the ratios Mo/Ce, Sb/Ce, Sn/Sm, Cd/Dy, W/U, and Rb/Tl in our data set, as these are expected to be relatively uniform in normal mid-ocean ridge basalts. Each ratio has an expected, "canonical" value in normal MORB based on prior work. For the most part, these canonical ratios are based on empirical observations of similar behavior in natural terrestrial samples. The complexities imposed on most of these elements by formation of the Earth's core makes a chondritic reference, for example, highly impractical because the silicate Earth is unlikely to have maintained chondritic ratios of these elements.

[24] For comparison with our data set for plume-influenced ridges, we also show data from *Jenner and O'Neill* [2012b], which is among the few studies to report a comprehensive data set for these elements in a large number of MORBs. For this comparison, both our data set and the samples from *Jenner and O'Neill* [2012b] have been filtered to yield data sets including only normal MORB (i.e., NMORB), as defined by a chondrite-normalized La/Sm ratio (i.e., La/Sm_N) of <1, that were collected on- or near-axis from active mid-ocean ridge spreading centers, far from known hotspot influences (this study n = 141; Jenner data n = 191). Data from seamounts, fracture zones, and back-arc spreading centers were excluded. We note some systematic differences in element concentrations between the *Jenner and O'Neill* [2012b] data set and ours (e.g., for Cd and Sb; Fig. 2b,d), which may be due to inter-laboratory biases related to differences in analytical methods (laser ablation ICP-MS vs. bulk dissolution) and calibration techniques. Specifically, we note that the *Jenner and O'Neill* [2012b] data set relies on a single, synthetic glass standard for external calibration (NIST 612 glass). *Jenner and O'Neill* [2012a] note that determinations of these elements in particular are less accurate than for more conventional trace elements, perhaps due to larger uncertainties in the composition of the NIST 612 glass for these elements. Unfortunately, the *Jenner and O'Neill* [2012b] data set contains only three samples in common with this work, so a fully comprehensive assessment of bias cannot presently be made.

[25] Figure 2 compares trace element abundances and ratios from our data set with NMORB and "canonical" ratios compiled from prior work (Mo/Ce = 0.034 [*Sun*, 2003], Sb/Ce = 0.0012 [*Sims et al*., 1990], Sn/Sm = 0.32 [*Jochum et al*., 1993], Cd/Dy = 0.027 [*Yi et al*., 2000], Rb/Tl = 230 [*Hertogen et al*., 1980], and W/U = 0.65 [*Arevalo and McDonough*, 2008]). This comparison shows reasonable agreement between the two NMORB data sets, with the exceptions of Cd and Sb as discussed above (Fig. 2b,d). Moreover, the majority of our NMORB data show clear fidelity with the canonical ratios Mo/Ce, Sb/Ce, Sn/Sm, Rb/Tl, and W/U, although there are obvious excursions in each ratio in our full data set that may relate to variations in mantle source composition or processes at or near mantle plumes (see below). The Cd/Dy ratio, however, does not conform to the global basalt ratio of 0.027 proposed by *Yi et al*. [2000] for either NMORB data set, which both indicate lower ratios of 0.017 or 0.014 (Fig. 2d). For the purposes of this discussion, the absolute value of the MORB Cd/Dy ratio is not a central issue, as our main purpose is to illustrate variations in these ratios as a function of hotspot proximity. We thus choose to also show an empirical reference ratio of Cd/Dy = 0.014 (average of our NMORB data) as a baseline against which tocompare the data. We also note that the Rb/Tl ratio cited for normal MORB [230; [*Hertogen et al*., 1980], although a fair average of our full data set, appears too high to represent thenormal MORB baseline, which may be closer to 100 or less. We thus also show a reference ratio of Rb/Tl = 115 (average Rb/Tl from the NMORB data of *Jenner and O'Neill* [2012b]) as an additional reference point (Fig. 2e).

4.2. Variations with Plume Proximity

[26] In the following discussion, we divide the mid-ocean ridge system into six regions (the north Atlantic, the Azores platform and equatorial Atlantic, the south Atlantic, the Easter microplate region, the Galápagos spreading center, and the Gulf of Aden;

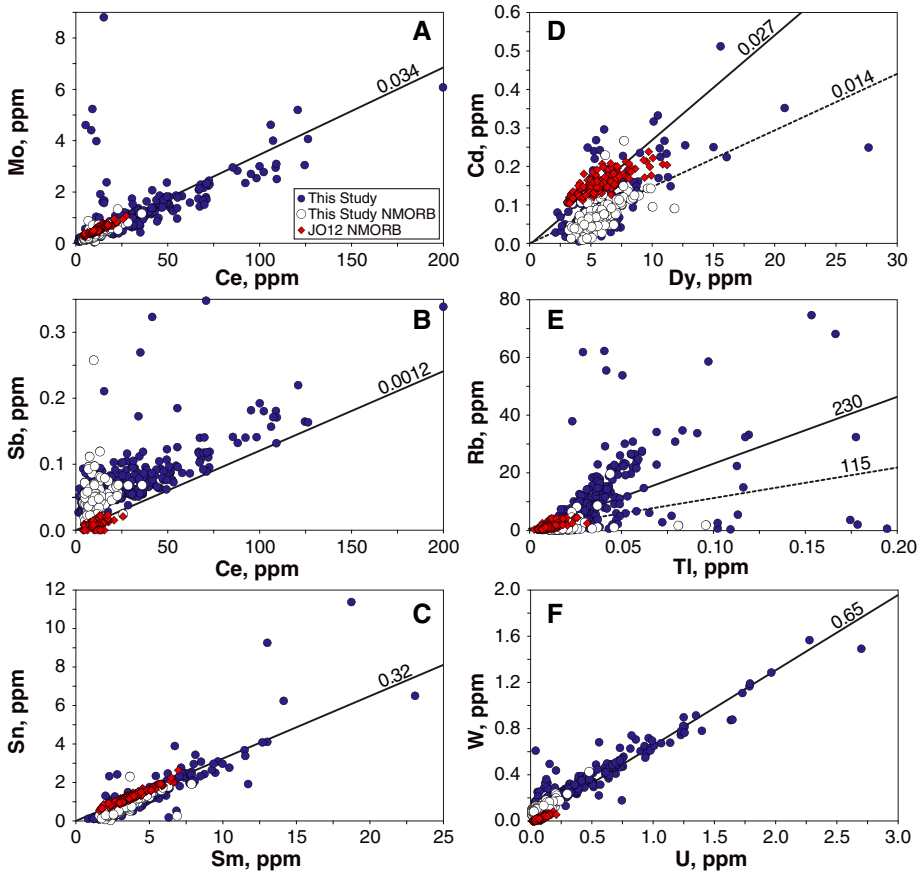

Figure 2. Plots of "unconventional" trace elements vs. trace elements expected to partition similarly during mantle melting and crystallization. Dark blue circles are the full data set from this study, open circles are data from this study filtered for NMORB only (see main text), red diamonds are NMORB data from *Jenner and O'Neill* [2012b]. (a) Mo vs. Ce, where the line indicates the expected NMORB Mo/Ce ratio of 0.034 [*Sun*, 2003], (b) Sb vs. Ce, where the line indicates the expected NMORB Sb/Ce ratio of 0.0012 [*Sims et al*., 1990], (c) Sn vs. Sm, where the line indicates the expected NMORB Sn/Sm ratio of 0.32 [*Jochum et al*., 1993], (d) Cd vs. Dy, where the solid line indicates the expected NMORB Cd/Dy ratio of 0.027 [*Yi et al*., 2000] and the dotted line indicates the empirical ratio of 0.014 (average of the NMORB data from this study), (e) Rb vs. Tl, where the solid line indicates the expected NMORB Rb/Tl ratio of 230 [*Hertogen et al*., 1980] and the dotted line indicates the empirical ratio of 115 (average of NMORB data from *Jenner and O'Neill* [2012b]), and (f) W vs. U, where the line indicates the expected NMORB W/U ratio of 0.65 [*Arevalo and McDonough*, 2008]. Note that the U data plotted here (and used for calculations of W/U ratio) are isotope dilution (Table 6), owing to the higher precision of that method.

Fig. 1), and discuss the variations in each ratio with proximity to known plume-related features along each ridge section.

4.2.1. North Atlantic (Iceland and Jan Mayen)

[27] The two predominant plume features along thenorthern Mid-Atlantic ridge are the Iceland and Jan Mayen hotspots (Fig. 1a). Mixing along the ridge between these trace element-enriched plume mantle sources and the ambient normal MORB mantle (present from 50-60°N [Reykjanes] and 66-70°N [Kolbeinsey]) is evident in the light rare earth elements (LREE; e.g., La/Sm_N; Fig. 3a). Dominant mixing gradients are visible from 60°N northwards along the Reykjanes ridge to Iceland, and from 72°-74°N on the Mohns ridge proximal to the Jan Mayen hotspot [e.g., *Schilling et al*., 1999]. North of 74°N is the Knipovich ridge, an unusual, slow-spreading region bordering the Svalbard continental shelf, contamination from which may drive LREE enrichment along this section of the MAR [*Schilling et al*., 1999].

[28] The Rb/Tl ratio tracks closely with variations inLa/Sm_N ratio (Fig. 3a-b). Rubidium and Tl are expected to have similar mantle/melt partition coefficients [*Sun and McDonough*, 1989], and fractionations in their ratio are thus most likely

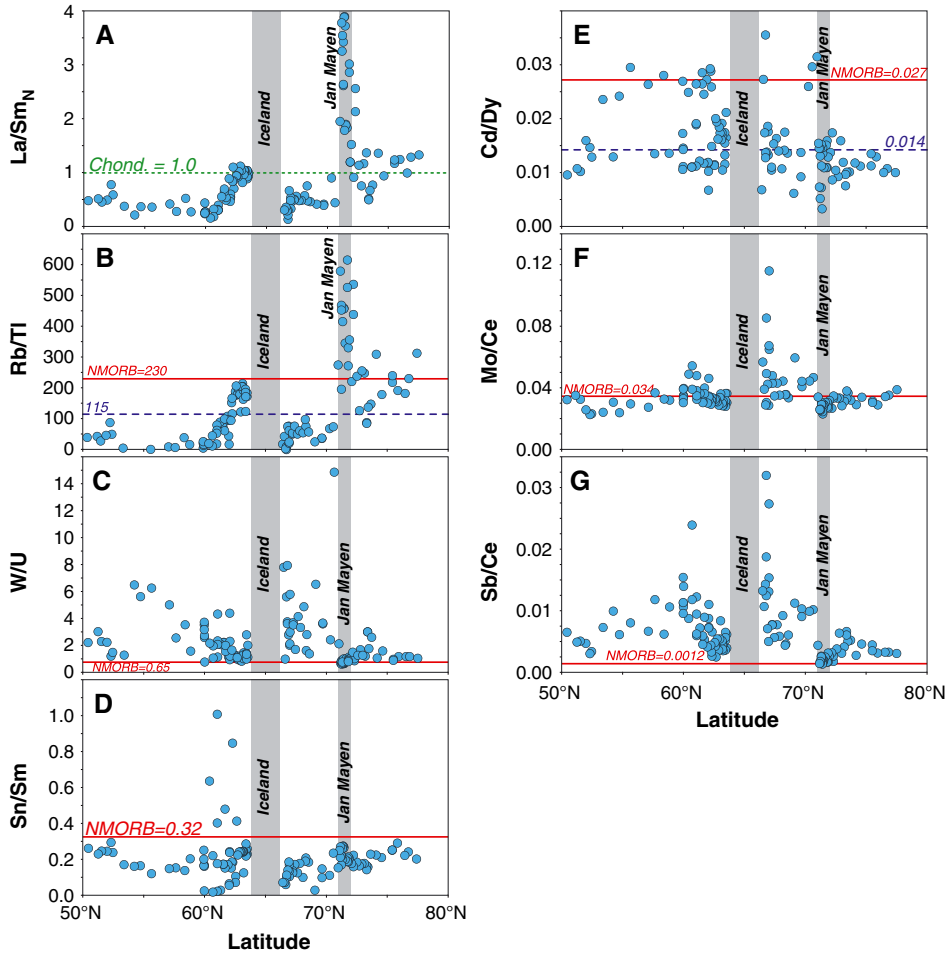

Figure 3. Trace element ratios vs. latitude along the Arctic and Reykjanes sections of the Mid-Atlantic ridge. Locations of the Jan Mayen and Iceland hotspots are indicated by vertical gray bars, and expected NMORB ratios, as identified in the text and on Figure 2, are indicated by horizontal, solid red lines (previously published values) and dashed blue lines (empirical values from this study). (a) Chondrite-normalized La/Sm ratio (i.e., La/Sm$_N$; normalized to chondrite of *Nakamura* [1974]), where the horizontal, dotted green line indicates a chondritic ratio of 1, segregating basalts with depleted light REE (<1) from those with enriched light REE (>1). (b) Rb/Tl ratio (note that the vertical scale is expanded to exclude the highest Rb/Tl samples, for clarity), (c) W/U ratio, (d) Sn/Sm ratio, (e) Cd/Dy ratio, (f) Mo/Ce ratio, and (g) Sb/Ce ratio.

reflective either of variations in the Rb/Tl ratio of the mantle source material, or of a role for sulfide in withholding or removing Tl from basaltic magmas. The close correspondence of Rb/Tl and La/Sm$_N$ ratios, however, more strongly suggests a source composition effect, as mantle sulfide will not influence the behavior of REE. The Sn/Sm ratio is relatively constant from 80°-50°N, with the exception of a few outliers. Enrichment in W/U ratio appears peripheral to the plume centers at Iceland and Jan Mayen and reaches maxima in regions of otherwise normal MORB, south of Iceland at ~55°N on the Reykjanes ridge, and between the two plumes at ~66°N on the Kolbeinsey ridge (Fig. 3c). Similar, though more subtle, trends may also be visible in the Mo/Ce, Sb/Ce, and Cd/Dy ratios(Fig. 3e-g). These local highs are outside the MORB-plume mixing zones that are well-defined by other trace element ratios (e.g., La/Sm$_N$, Rb/Tl; Fig. 3a-b), and are indistinguishable in most other geochemical traits from normal MORB. As discussed in the sections that follow, peripheral enrichments in W/U and Mo/Ce ratios are evident at each of the plume-ridge settings explored by this paper. These far-field enrichments in siderophile elements may signify a previously unrecognized plume signature that manifests at different length scales than the "classic" enrichments in lithophile trace elements that are often traditionally linked with plumes.

4.2.2. Azores Platform and Equatorial Atlantic (Sierra Leone)

[29] Proceeding south along the Mid-Atlantic ridge, the Azores platform (~34°-49°N) represents a broad zone of influence from the Azores plume, which is centered just east of the ridge at ~39°N. Further south, on the equatorial MAR, lies a trace element- and isotopically-enriched province centered at 1.7°N that has been linked to influence from the Sierra Leone mantle plume [*Schilling et al.*, 1994]. Note that these regions are not continuous along the MAR, but are juxtaposed in this discussion and on Figure 4 for the sake of efficiency. Both the Azores and Sierra Leone regions show classic signatures of plume influence in trace element geochemistry (e.g., elevated La/Sm_N; Fig. 4a), and indicate mixing of enriched plume sources with neighboring normal MORB adjacent to the plume centers.

[30] Crossing both of these plumes, little variation is evident in Sn/Sm or Cd/Dy ratios (Fig. 4d-e), although the Rb/Tl ratio closely mirrors the La/Sm_N ratio as noted above for the northern MAR (Fig. 4a-b). There are also mild enrichments of W/U, Mo/Ce, and Sb/Ce ratios crossing the Azores platform, particularly in a few samples south of 35°N (Fig. 4c, f-g). These three ratios also vary crossing the Sierra Leone plume, where the plume center shows overall lower ratios, but some samples show enrichment in W/U, Mo/Ce, and Sb/Ce to both the north and south of the plume center (Fig. 4c, f-g).

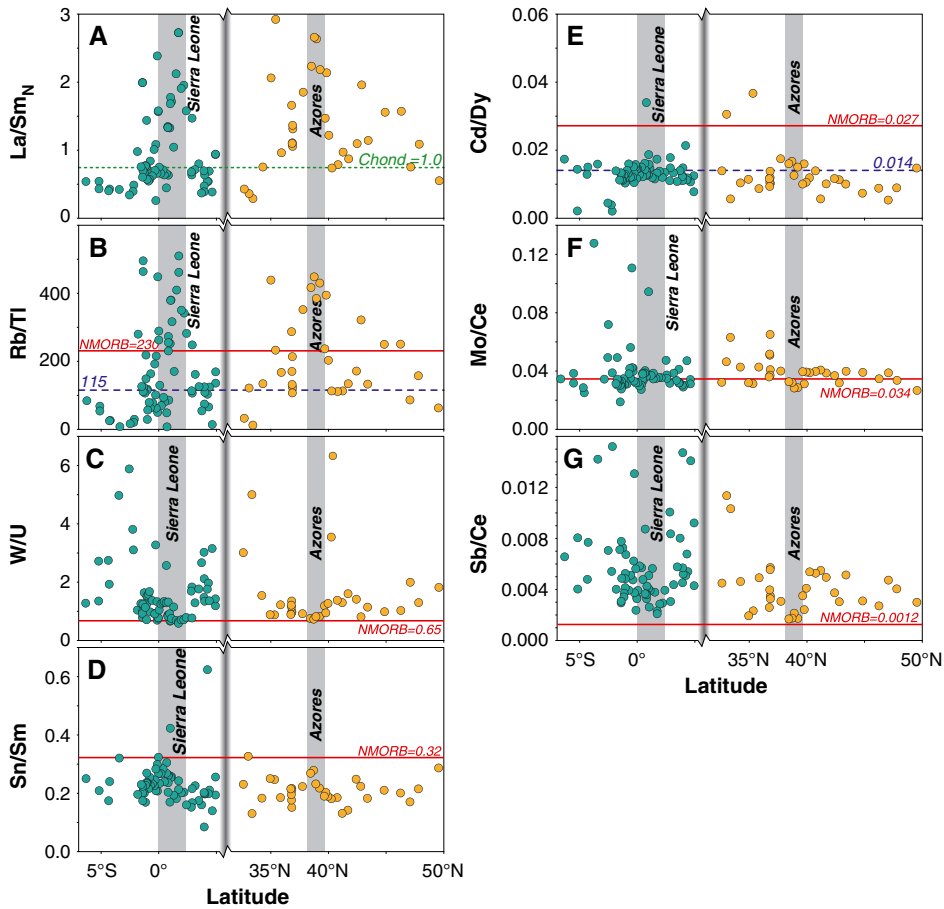

Figure 4. Trace element ratios vs. latitude along the Azores platform and Equatorial sections of the Mid-Atlantic ridge. Note the discontinuity in latitude along the abscissa, marked by a shaded vertical bar, which spans a gap in latitude from 5°N to 32°N. Locations of the Azores and Sierra Leone hotspots are indicated by vertical gray bars, and expected NMORB ratios, as identified in the text and on Figure 2, are indicated by horizontal, solid red lines (previously published values) and dashed blue lines (empirical values from this study). (a) Chondrite-normalized La/Sm ratio (i.e., La/Sm_N; normalized to chondrite of *Nakamura* [1974]), where the horizontal, dotted green line indicates a chondritic ratio of 1, segregating basalts with depleted light REE (<1) from those with enriched light REE (>1). (b) Rb/Tl ratio, (c) W/U ratio, (d) Sn/Sm ratio, (e) Cd/Dy ratio, (f) Mo/Ce ratio, and (g) Sb/Ce ratio.

4.2.3. South Atlantic (Ascension, St. Helena, Tristan de Cunha, Shona, Discovery, Bouvet)

[31] The southern MAR is peppered with influence from several on- and off-axis hotspots. Influences from off-axis plumes include Ascension (~9°S), St. Helena (~15°S), Tristan de Cunha (~37°S), and Discovery (~48°S), whereas the Shona plume is apparently on-axis (~52°S) and the Bouvet plume/triple junction (~55°S) marks the southern termination of the Mid-Atlantic ridge. Each of these plumes is visible in the geochemistry of MAR lavas, as shown for example by enrichments in the La/Sm_N ratio (Fig. 5a), which mixes back to normal MORB La/Sm_N ratios (<1) between plumes.

[32] Similar to the northern through equatorial MAR, along-strike variations in La/Sm_N ratio are closely paralleled by the Rb/Tl ratio (Fig. 5a-b), whereas Sn/Sm, Cd/Dy, and Sb/Ce are relatively constant along strike of this portion of the MAR (Fig. 5d-f, g). Enrichments in W/U (i.e., W/U>2), however, are evident between plume centers along the southern MAR, particularly between Shona and Discovery, between Discovery and Tristan de Cunha, between Tristan de Cunha and St. Helena, and a few samples between St. Helena and Ascension, whereas samples from the zones of peak influence of these plumes on the southern MAR have W/U ratios <2 (Fig. 5c). A similar, though subtler, pattern may be evident in the Mo/Ce ratio along the southern MAR (Fig. 5f).

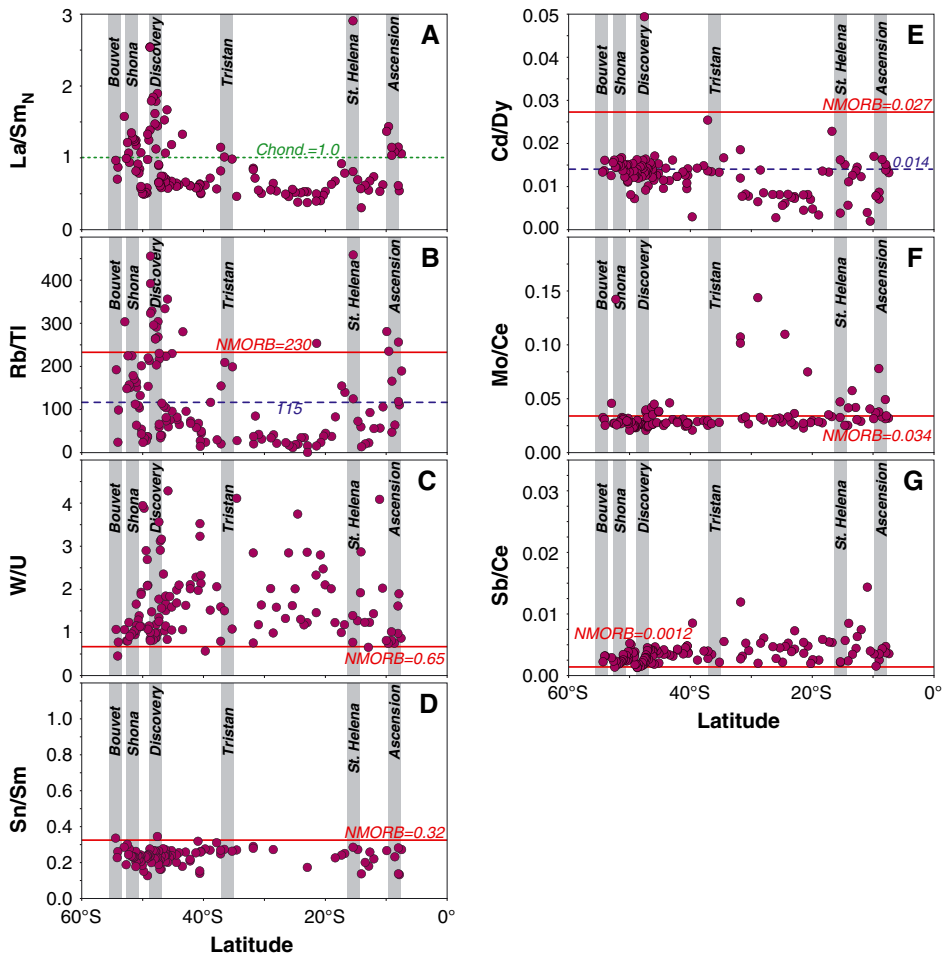

Figure 5. Trace element ratios vs. latitude along the southern section of the Mid-Atlantic ridge. Locations of the Ascension, St. Helena, Tristan de Cunha, Discovery, Shona, and Bouvet hotspots are indicated by vertical gray bars, and expected NMORB ratios, as identified in the text and on Figure 2, are indicated by horizontal, solid red lines (previously published values) and dashed blue lines. (a) Chondrite-normalized La/Sm ratio (i.e., La/Sm_N; normalized to chondrite of *Nakamura* [1974]), where the horizontal, dotted green line indicates a chondritic ratio of 1, segregating basalts with depleted light REE (<1) from those with enriched light REE (>1). (b) Rb/Tl ratio, (c) W/U ratio, (d) Sn/Sm ratio, (e) Cd/Dy ratio, (f) Mo/Ce ratio (note that the vertical scale is expanded to exclude the highest Mo/Ce samples, for clarity), and (g) Sb/Ce ratio.

4.2.4. Easter Microplate and Salas y Gomez Seamounts

[33] Along the East Pacific rise, the Easter microplate (~23°-28°S) and the associated eastward-trending Easter-Salas y Gomez seamount chain (~112°-103°W) show geochemical signatures consistent with binary mixing of MORB mantle with an enriched, plume-related source [e.g., *Fontignie and Schilling*, 1991; *Hanan and Schilling*, 1989; *Kingsley and Schilling*, 1998; *Kingsley et al.*, 2007; *Schilling et al.*, 1985]. Based on trace element and isotopic trends, the Salas y Gomez hotspot is hypothesized to be centered beneath the seamount chain near Salas y Gomez island (~105°-106°W), to the east of the EPR and the Easter microplate. Geochemical trends along-strike of the East Pacific rise (N-S) are shown in Supplementary Figure 1. Variations in La/Sm_N ratio, plotted along-strike of the seamount chain (E-W), show enrichments in LREE towards the east, reaching a maximum at the postulated hotspot center (Fig. 6a), but La/Sm_N mixes towards normal MORB ratios <1 towards the microplate rift zones and EPR in the west.

[34] In this region, the Rb/Tl ratio shows along-strike variation similar to that shown by La/Sm_N (Fig. 6a-b). The Mo/Ce ratio appears relatively invariant with proximity to the plume, although a

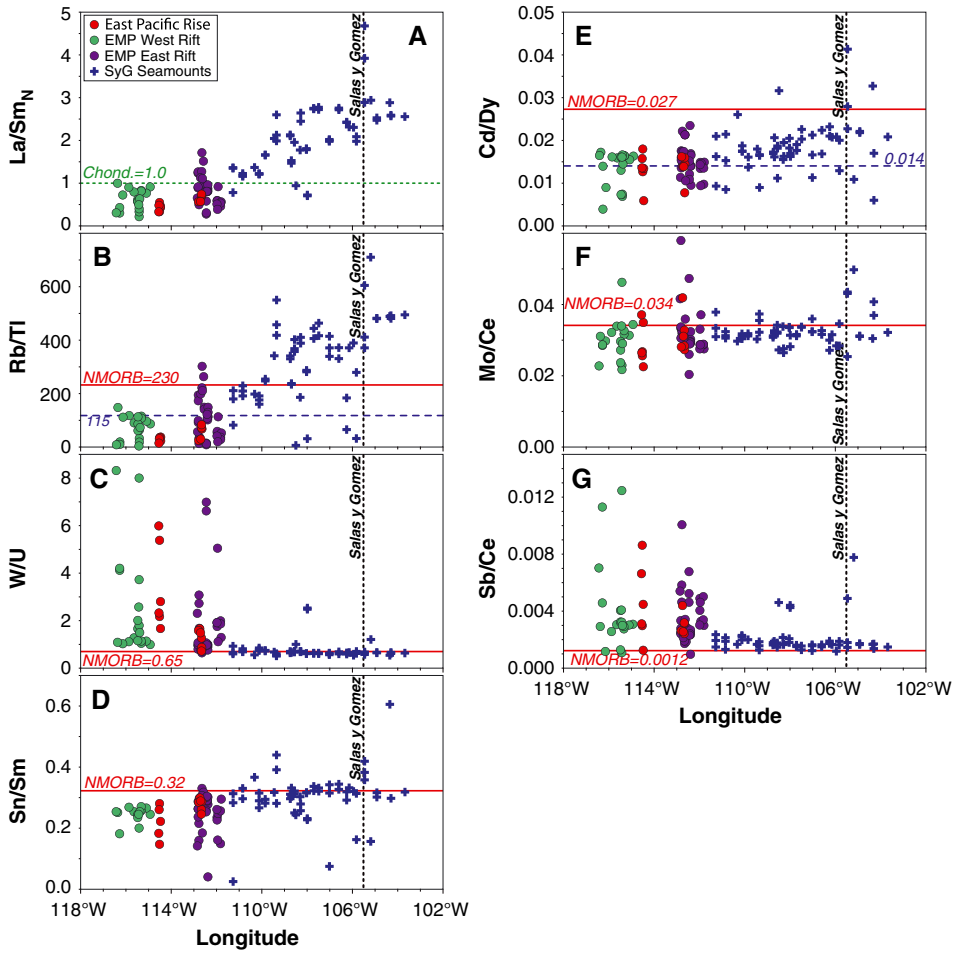

Figure 6. Trace element ratios vs. longitude across the Easter-Salas y Gomez section of the East Pacific rise. Symbols are coded for location as shown on Figure 1; EPR and microplate samples are colored circles, Salas y Gomez seamount chain samples are blue crosses. Expected NMORB ratios, as identified in the text and on Figure 2, are indicated by horizontal, solid red lines (previously published values) and dashed blue lines (empirical values from this study). (a) Chondrite-normalized La/Sm ratio (i.e., La/Sm_N; normalized to chondrite of *Nakamura* [1974]), where the horizontal, dotted green line indicates a chondritic ratio of 1, segregating basalts with depleted light REE (<1) from those with enriched light REE (>1). (b) Rb/Tl ratio, (c) W/U ratio, (d) Sn/Sm ratio, (e) Cd/Dy ratio, (f) Mo/Ce ratio, and (g) Sb/Ce ratio.

few enriched samples are evident in the Easter microplate region (Fig. 6f). Conversely, the W/U and Sb/Ce ratios are significantly elevated in the Easter microplate rift zone lavas and the EPR lavas west of the hotspot, although the seamounts themselves show little to no enrichment in these ratios. Interestingly, the Cd/Dy and Sn/Sm ratios are mildly elevated in the Easter-Salas y Gomez seamounts, despite remaining relatively constant and low along the EPR and microplate rift zones. A high Cd/Dy ratio may signify a higher mean pressure of melting, and a greater role for garnet in the mantle source, beneath the Easter-Salas y Gomez seamounts relative to the nearby microplate rifts and EPR. A high Sn/Sm ratio may signify a specific enrichment in Sn for the Salas y Gomez plume source.

4.2.5. Galápagos Spreading Center

[35] In the equatorial Pacific, the Galápagos spreading center sits just north of the present location of the Galápagos hotspot. The spreading center itself is offset by several prominent fracture zones, the most significant of which (for this discussion) are the fracture zones at 91°W and 95.5°W. The influence of Galápagos plume-related mantle on the spreading center basalts (e.g., as shown by La/Sm_N ratio; Fig. 7a) peaks near the fracture zone at 91°W, which is almost due north of the present Galápagos hotspot center, and the fracture zone at 95.5°W segregates strongly plume-influenced basalts to the east from normal MORB-like basalts to the west [e.g., *Schilling et al.*, 2003; *Schilling et al.*, 1976; *Schilling et al.*, 1982].

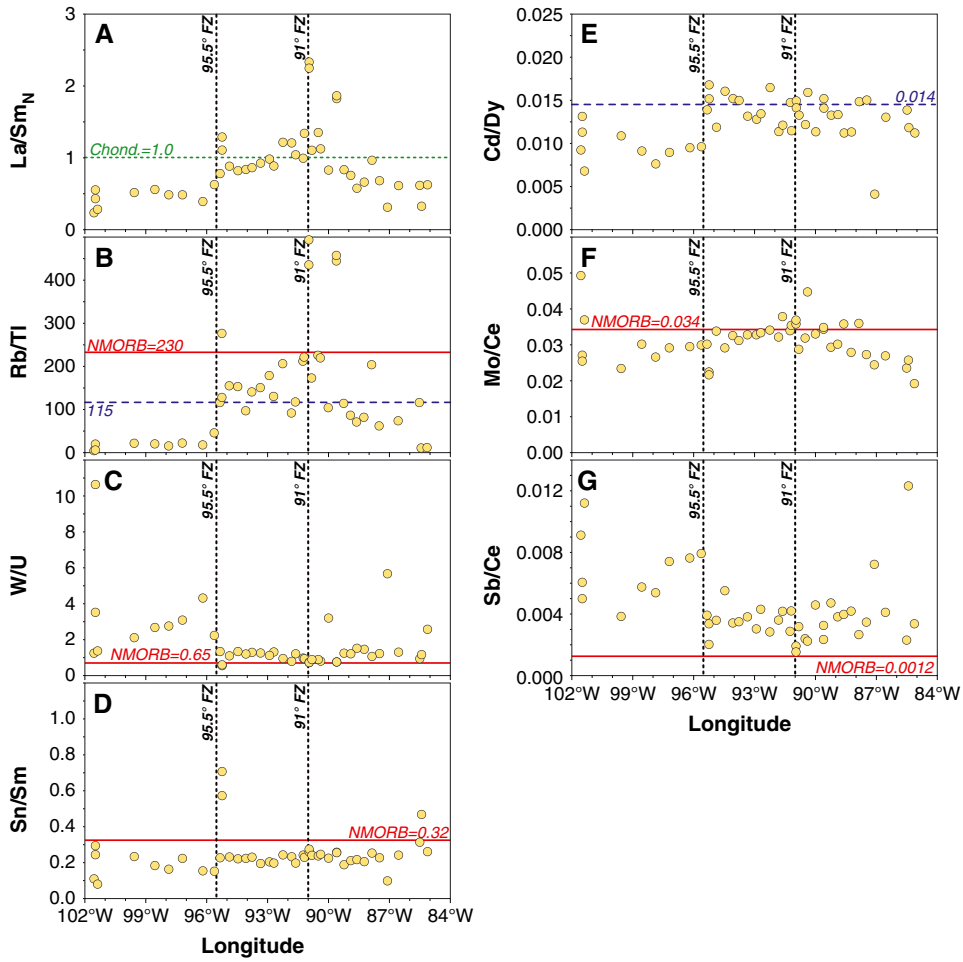

Figure 7. Trace element ratios vs. longitude along the Galápagos spreading center. Locations of the fracture zones at 91°W and 95.5°W are indicated by vertical dashed lines, and expected NMORB ratios, as identified in the text and on Figure 2, are indicated by horizontal, solid red lines (previously published values) and dashed blue lines (empirical values from this study). (a) Chondrite-normalized La/Sm ratio (i.e., La/Sm_N; normalized to chondrite of *Nakamura* [1974]), where the horizontal, dotted green line indicates a chondritic ratio of 1, segregating basalts with depleted light REE (<1) from those with enriched light REE (>1). (b) Rb/Tl ratio, (c) W/U ratio, (d) Sn/Sm ratio, (e) Cd/Dy ratio, (f) Mo/Ce ratio, and (g) Sb/Ce ratio.

[36] As noted above for several other regions, Sn/Sm and Mo/Ce do not vary significantly along strike of the Galápagos spreading center (Fig. 7d, f), and the Rb/Tl ratio shows variations very similar to La/Sm_N (Fig. 7a-b). The Cd/Dy ratio is lower west of the 95.5°W fracture zone (Fig. 7e), possibly signifying a diminished role for garnet in the mantle source away from the strongest plume influence. The W/U and, more subtly, the Sb/Ce ratios are also elevated west of the 95.5°W fracture zone, away from the plume center, which has lower W/U and Sb/Ce (Fig. 7c, g).

4.2.6. Gulf of Aden and Asal Rift

[37] Sea-floor spreading and rifting in the Gulf of Aden-Gulf of Tadjoura-Asal rift system is one expression of the continental rifting taking place in eastern Africa, associated with the impingement of the Afar hotspot on the African continent. Geochemical domain boundaries were first identified by *Schilling et al.* [1992] at 44°E, separating enriched lavas from the Asal rift and Gulf of Tajdoura from even more enriched lavas of the west Sheba ridge, and at 48°E, separating trace element- and isotopically-enriched basalts to the west from relatively depleted, normal MORB to the east. The domains to the west and east of 44°E both show enriched, although distinct, geochemical signatures (e.g., variably elevated La/Sm_N; Fig. 8a). *Schilling et al.* [1992] interpreted these enrichments as representing signatures of the regional continental lithosphere through which rifting has occurred (west of 44°E,

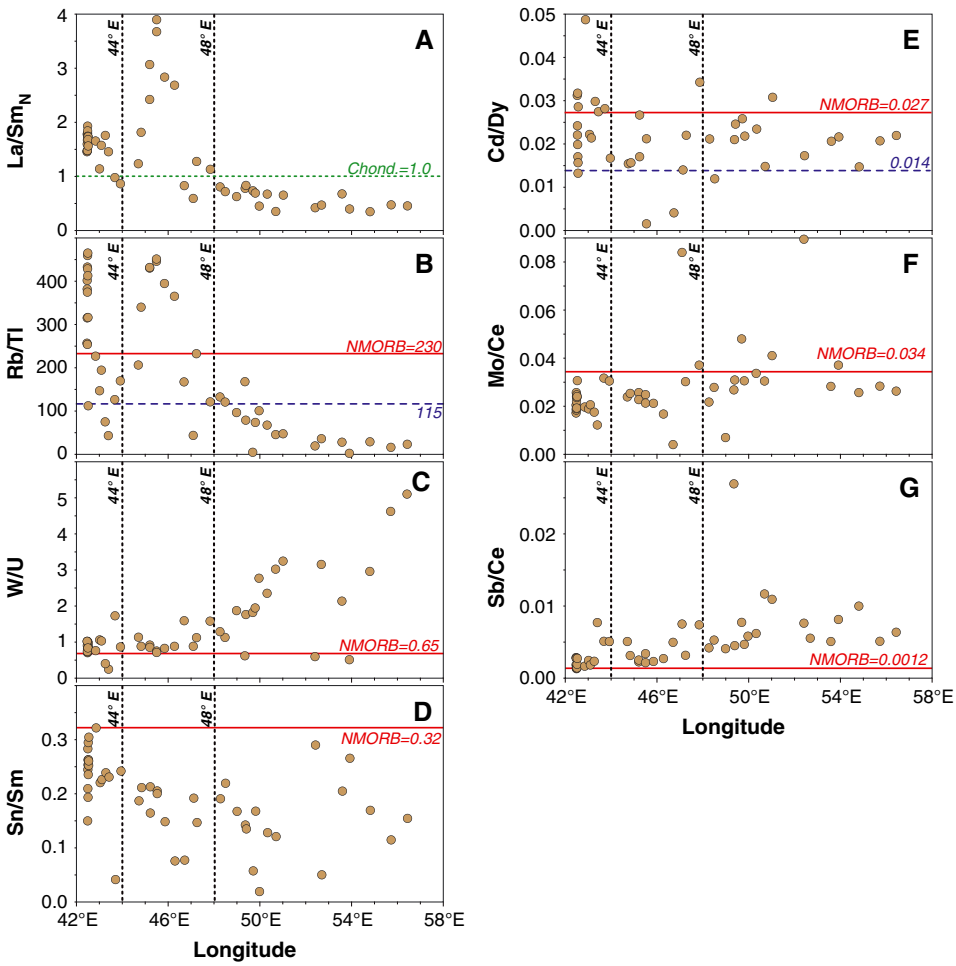

Figure 8. Trace element ratios vs. longitude along the Gulf of Aden, Gulf of Tadjoura, and Asal rift. Locations of geochemical divisions at 44°E and 48°E, from *Schilling et al.* [1992], are indicated by vertical dashed lines, and expected NMORB ratios, as identified in the text and on Figure 2, are indicated by horizontal, solid red lines (previously published values) and dashed blue lines (empirical values from this study). (a) Chondrite-normalized La/Sm ratio (i.e., La/Sm_N; normalized to chondrite of *Nakamura* [1974]), where the horizontal, dotted green line indicates a chondritic ratio of 1, segregating basalts with depleted light REE (< 1) from those with enriched light REE (> 1). (b) Rb/Tl ratio, (c) W/U ratio, (d) Sn/Sm ratio, (e) Cd/Dy ratio, (f) Mo/Ce ratio, and (g) Sb/Ce ratio.

in the Gulf of Tadjoura and Asal rift), and of the Afar plume, which is most evident at ~46°E.

[38] Along strike, the Rb/Tl ratio closely parallels the trends in La/Sm_N ratio, with significant elevation of both ratios in the west, decreasing to local minima east of 48°E, although enrichment in Rb/Tl in the farthest west Asal rift lavas is significantly higher than indicated by La/Sm_N (Fig. 8a-b). Conversely, W/U, Mo/Ce, and Sb/Ce are all lowest in the west, closest to the continent and the plume, and increase eastwards with distance from the predominant plume signature (Figs. 8c, f-g). No significant along-strike trends are apparent in Sn/Sm or Cd/Dy ratios (Fig. 8d-e).

4.2.7. Global Systematics

[39] Though the above discussion is segregated geographically, a few common threads among these regions also permit some more general observations. For example, global variations in the Rb/Tl ratio track closely with light REE enrichment, as indicated by the La/Sm_N ratio (Figs. 3a-b to 8a-b). Globally, La/Sm_N and Rb/Tl show a strong, positive, and approximately linear correlation (Fig. 9a), suggesting the utility of this ratio as a sensor of overall incompatible element enrichment in mantle sources.

[40] We also observe enrichments in the W/U ratio over the expected normal MORB/bulk silicate Earth value of 0.65, which has otherwise been shown to be relatively invariant in terrestrial igneous rocks [*Arevalo and McDonough*, 2008]. Interestingly, however, higher W/U ratios are not coincident with the geographic centers of plume-related features on these ridges. Instead, the most plume-like samples (e.g., LREE enriched) have low W/U, but the ratio is higher with distance from the inferred plumes (Figs. 3c-8c), such that the highest W/U ratios appear proximal to plumes, but not at their centers. In some instances this trend is mirrored more subtly in Mo/Ce and Sb/Ce ratios. The W/U ratio (and to a lesser extent, Mo/Ce and Sb/Ce ratios) is inversely correlated with La/Sm_N ratio (Fig. 9b-d), and W/U ratios >2 are restricted exclusively to a subset of basalts with $La/Sm_N \leq 1$ (i.e., some, but not all, NMORBs). These signals might provide evidence for peripheral entrainment of W-enriched, lower mantle material by upwelling mantle plumes. During ascent, upwelling plumes may entrain adjacent mantle material in the overall solid flow field, and isotopic signatures of plume-related lavas at global ocean islands provide substantial evidence in favor of this process [e.g., *Hart et al.*, 1992]. Such entrained mantle may be compositionally unrelated to the plume material that feeds the primary heads and conduits of plumes, which are often interpreted to originate from

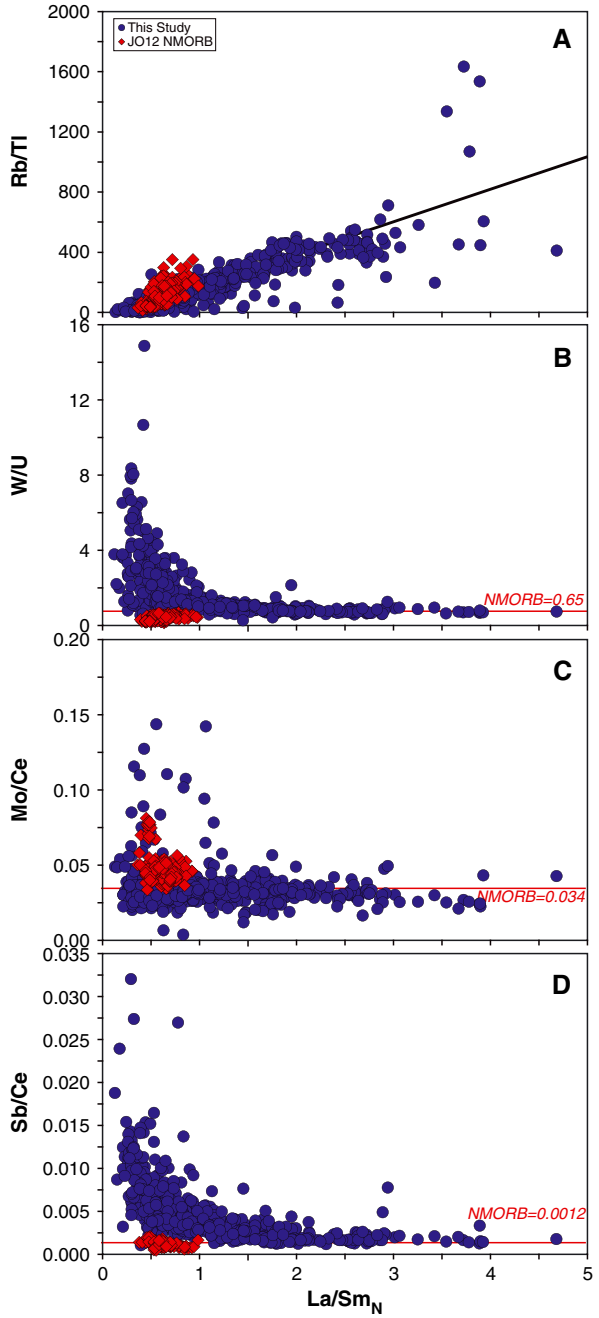

Figure 9. Trace element ratios vs. chondrite-normalized La/Sm ratio (i.e., La/Sm_N; normalized to chondrite of *Nakamura* [1974]). Dark blue circles are data from this study, red diamonds are NMORB data from *Jenner and O'Neill* [2012b]. Horizontal red lines indicate expected NMORB ratios from *Arevalo and McDonough* [2008] and *Sun* [2003]. (a) Rb/Tl ratio vs. La/Sm_N. The heavy black line is a least-squares linear regression through the data from this study ($y = 216.010x - 60.148$; $r^2 = 0.6987$). (b) W/U, (c) Mo/Ce, and (d) Sb/Ce vs. La/Sm_N.

deeply-recycled subducted materials, but might represent the ambient mantle adjacent to the point of plume initiation. Tungsten, Mo, and Sb are all expected to be enriched in the Earth's core relative to the silicate mantle, and mantle that has incorporated a small component of core material would thus be relatively enriched in these elements over their strictly lithophile counterparts, U and Ce. We note, however, that these data do not exclude plumes themselves from containing an elevated W (or Mo or Sb) signature from the core-mantle boundary. Rather, elevations in the W/U ratio arising from contributions of W-enriched core material are only resolvable in instances where either the contribution from the core is large (1 wt.% for average depleted MORB mantle, or more for sources originally enriched in W; *Arevalo and McDonough* [2008]) or the mantle W content is low (i.e., strongly depleted mantle). These contributions may thus be present throughout mantle plumes, but are only resolvable peripherally where the mantle is more depleted. Mantle that is otherwise geochemically similar to NMORB, but enriched in W, may signify peridotite that was resident near the core-mantle boundary prior to peripheral entrainment by a neighboring plume. In such a case, one might expect a correlation between elevated $^{3}He/^{4}He$ ratios and elevated W/U ratios, as both are potentially indicative of source material derived from the lower mantle. An overall paucity of helium isotope data for samples with high W/U ratio, however, makes a global assessment impractical at present, although this is a direction that is ripe for future work.

5. Summary

[41] New trace element data for a global suite of plume-influenced mid-ocean ridge basalts show variations in lesser-examined trace element ratios as a function of proximity to plume influence. The new data show that the Rb/Tl ratio closely mirrors the La/Sm_N ratio, such that the two ratios show an approximately linear correlation, and Rb/Tl thus provides a sensitive tracer of plume-related, enriched mantle domains. The W/U ratio may be sensitive to enrichment related to interactions near the Earth's core. We find that W/U is not elevated at plume centers, but significant enrichments in W/U, and to a lesser extent the Mo/Ce and Sb/Ce ratios, are present at mid-ocean ridges proximal to plumes. Such enrichments may provide evidence of far-field entrainment of lower mantle material that has interacted with the core by deeply-rooted, upwelling mantle plumes.

Acknowledgements

[42] Thanks to Tyrone Rooney for a thorough, thoughtful, and constructive review, Charlie Langmuir and Allie Gale for spurring progress on this manuscript, and to Sylvia Savage for her patience in advance of submission. Kerstin Lehnert and the excellent support staff at IEDA/PetDB, and Leslie Hsu in particular, provided essential guidance on the organization and documentation of the data set. Steve Carey and the curatorial assistants at MGSL at GSO/URI also provided key assistance with sample registration, and the long-term maintenance of the MGSL rock collection. NSF award OCE-9528801 to J.G. S. supported trace element analyses of glass and lava samples. K.K. gratefully acknowledges NSF award MARGINS-EAR-0841108 and the Deep Carbon Observatory's Reservoirs and Fluxes Directorate, which supported the organization of data and preparation of this manuscript. NSF award OCE-0644625 provides curatorial support for marine geological samples at the University of Rhode Island.

References

Agranier, A., J. Blichert-Toft, D. Graham, V. Debaille, P. Schiano, and F. Albaréde (2005), The spectra of isotopic heterogeneities along the mid-Atlantic Ridge, *Earth Planet Sci. Lett.*, *238*, 96–109, doi:10.1016/j.epsl.2005.07.011.

Anderson, R. N., D. A. Clague, K. D. Klitgord, M. Marshall, and R. K. Nishimori (1975), Magnetic and Petrologic Variations along the Galapagos Spreading Center and Their Relation to the Galapagos Melting Anomaly, *Geol. Soc.Am. Bull.*, *86*(5), 683–694.

Andres, M., J. Blichert-Toft, and J.-G. Schilling (2002), Hafnium isotopes in basalts from the southern Mid-Atlantic Ridge from 40°S to 55°S: Discovery and Shona plume-ridge interactions and the role of recycled sediments, *Geochem. Geophys. Geosyst.*, *3*(10), 8502, doi:10.1029/2002gc000324.

Andres, M., J. Blichert-Toft, and J.-G. Schilling (2004), Nature of the depleted upper mantle beneath the Atlantic: evidence from Hf isotopes in normal mid-ocean ridge basalts from 79°N to 55°S, *Earth Planet Sci. Lett.*, *225*(1–2), 89–103, doi:10.1016/j.epsl.2004.05.041.

Arevalo, R., and W. F. McDonough (2008), Tungsten geochemistry and implications for understanding the Earth's interior, *Earth Planet Sci. Lett.*, *272*(3–4), 656–665, doi:10.1016/j.epsl.2008.05.031.

Bäcker, H., M. Clin, and K. Lange (1973), Tectonics in the Gulf of Tadjura, *Marine Geology*, *15*(5), 309–327, doi:10.1016/0025-3227(73)90048-0.

Bézos, A., and E. Humler (2005), The $Fe^{+3}/\sum Fe$ ratios of MORB glasses and their implications for mantle melting, *Geochim. Cosmochim. Acta*, *69*(3), 711–725, doi:10.1016/j.gca.2004.07.026.

Blichert-Toft, J., A. Agranier, M. Andres, R. Kingsley, J.-G. Schilling, and F. Albaréde (2005), Geochemical segmentation of the Mid-Atlantic Ridge north of Iceland and ridge-hot spot interaction in the North Atlantic, *Geochem. Geophys. Geosyst.*, *6*(1), Q01E19, doi:10.1029/2004gc000788.

gault, H., L. Dmitriev, J. G. Schilling, A. Sobolev, J. L. Joron, and H. D. Needham (1988), Mantle heterogeneity from trace elements: MAR triple junction near 14°N, *Earth Planet Sci. Lett.*, *88*(1–2), 27–36, doi:10.1016/0012-821x(88)90043-x.

Bryan, W. B., and J. G. Moore (1977), Compositional variations of young basalts in the Mid-Atlantic Ridge rift valley near lat 36°49'N, *Geol. Soc.Am. Bull.*, *88*(4), 556–570.

Bryan, W. B., G. Thompson, and P. J. Michael (1979), Compositional variation in a steady-state zoned magma chamber: Mid-Atlantic Ridge at 36°50'N, *Tectonophysics*, *55*(1–2), 63–85, doi:10.1016/0040-1951(79)90335-4.

Christie, D. M., I. S. E. Carmichael, and C. H. Langmuir (1986), Oxidation states of mid-ocean ridge basalt glasses, *Earth Planet Sci. Lett.*, *79*, 397–411.

Cohen, R. S., and R. K. O'Nions (1982), The Lead, Neodymium and Strontium Isotopic Structure of Ocean Ridge Basalts, *J. Petrol.*, *23*(3), 299–324.

Dixon, J. E., L. Leist, C. H. Langmuir, and J.-G. Schilling (2002), Recycled dehydrated lithosphere observed in plume-influenced mid-ocean-ridge basalt, *Nature*, *420*, 385–389.

Dosso, L., H. Bougault, and J.-L. Joron (1993), Geochemical morphology of the North Mid-Atlantic Ridge, 10°-24°N: Trace element-isotope complementarity, *Earth Planet Sci. Lett.*, *120*, 443–462, doi:10.1016/0012-821x(93)90256-9.

Dosso, L., B. B. Hanan, H. Bougault, J.-G. Schilling, and J.-L. Joron (1991), Sr-Nd-Pb geochemical morphology between 10° and 17°N on the Mid-Atlantic Ridge: A new MORB isotope signature, *Earth Planet Sci. Lett.*, *106*(1–4), 29–43, doi:10.1016/0012-821x(91)90061-l.

Douglass, J., J.-G. Schilling, and D. Fontignie (1999), Plume-ridge interactions of the Discovery and Shona mantle plumes with the southern Mid-Atlantic Ridge (40°-55°S), *J. Geophys. Res.*, *104*(B2), 2941–2962, doi:10.1029/98jb02642.

Eggins, S., J. D. Woodhead, L. P. J. Kinsley, G. E. Mortimer, P. Sylvester, M. T. McCulloch, J. M. Hergt, and M. R. Handler (1997), A simple method for the precise determination of >40 trace elements in geological samples by ICPMS using enriched isotope internal standardisation, *Chem. Geol.*, *134*(4), 311–326.

Eiler, J. M., P. Schiano, N. Kitchen, and E. M. Stolper (2000), Oxygen-isotope evidence for recycled crust in the sources of mid-ocean-ridge basalts, *Nature*, *403*(6769), 530–534, doi:10.1038/35000553.

Elkins, L. J., et al. (2011), Understanding melt generation beneath the slow-spreading Kolbeinsey Ridge using ^{238}U, ^{230}Th, and ^{231}Pa excesses, *Geochim. Cosmochim. Acta*, *75*(21), 6300–6329, doi:10.1016/j.gca.2011.08.020.

Fisk, M. R., A. E. Bence, and J. G. Schilling (1982), Major element chemistry of Galapagos Rift Zone magmas and their phenocrysts, *Earth Planet Sci. Lett.*, *61*(1), 171–189, doi:10.1016/0012-821x(82)90050-4.

Fontignie, D., and J. G. Schilling (1991), ^{87}Sr/^{86}Sr and REE variations along the Easter Microplate boundaries (south Pacific): Application of multivariate statistical analyses to ridge segmentation, *Chem. Geol.*, *89*(3–4), 209–241, doi:10.1016/0009-2541(91)90018-m.

Fontignie, D., and J.-G. Schilling (1996), Mantle heterogeneities beneath the South Atlantic: a Nd-Sr-Pb isotope study along the Mid-Atlantic Ridge (3°S-46°S), *Earth Planet Sci. Lett.*, *142*(1–2), 209–221, doi:10.1016/0012-821x(96)00079-9.

Graham, D. W., W. J. Jenkins, J.-G. Schilling, G. Thompson, M. D. Kurz, and S. E. Humphris (1992), Helium isotope geochemistry of mid-ocean ridge basalts from the South Atlantic, *Earth Planet Sci. Lett.*, *110*(1–4), 133–147, doi:10.1016/0012-821x(92)90044-v.

Hanan, B. B., and J.-G. Schilling (1989), Easter Microplate Evolution: Pb Isotope Evidence, *J. Geophys. Res.*, *94*(B6), 7432–7448, doi:10.1029/JB094iB06p07432.

Hanan, B. B., R. H. Kingsley, and J. G. Schilling (1986), Pb isotope evidence in the South Atlantic for migrating ridge-hotspot interactions, *Nature*, *322*(6075), 137–144.

Hanan, B. B., J. Blichert-Toft, R. Kingsley, and J. G. Schilling (2000), Depleted Iceland mantle plume geochemical signature: Artifact of multicomponent mixing?, *Geochem. Geophys. Geosyst.*, *1*(4), 1–19, doi:10.1029/1999gc000009.

Hannigan, R. E., A. R. Basu, and F. Teichmann (2001), Mantle reservoir geochemistry from statistical analysis of ICP-MS trace element data of equatorial mid-Atlantic MORB glasses, *Chem. Geol.*, *175*(3–4), 397–428, doi:10.1016/s0009-2541(00)00335-1.

Hart, S. R., J.-G. Schilling, and J. L. Powell (1973), Basalts from Iceland and Along the Reykjanes Ridge: Sr Isotope Geochemistry, *Nature*, *246*, 104–107, doi:10.1038/physci246104a0.

Hart, S. R., E. H. Hauri, L. A. Oschmann, and J. A. Whitehead (1992), Mantle plumes and entrainment: Isotopic evidence, *Science*, *256*(5056), 517–520, doi:10.1126/science.256.5056.517.

Hékinian, R., D. Bideau, R. Hébert, and Y. Niu (1995), Magmatism in the Garrett transform fault (East Pacific Rise near 13°27'S), *J. Geophys. Res.*, *100*(B6), 10163–10185, doi:10.1029/94jb02125.

Hémond, C., A. W. Hofmann, I. Vlastélic, and F. Nauret (2006), Origin of MORB enrichment and relative trace element compatibilities along the Mid-Atlantic Ridge between 10° and 24°N, *Geochem. Geophys. Geosyst.*, *7*(12), Q12010, doi:10.1029/2006gc001317.

Hermes, O. D., and J. G. Schilling (1976), Olivine from Reykjanes ridge and Iceland tholeiites, and its significance to the two-mantle source model, *Earth Planet Sci. Lett.*, *28*(3), 345–355, doi:10.1016/0012-821x(76)90196-5.

Hertogen, J., M. J. Janssens, and H. Palme (1980), Trace elements in ocean ridge basalt glasses: implications for fractionations during mantle evolution and petrogenesis, *Geochim. Cosmochim. Acta*, *44*(12), 2125–2143, doi:10.1016/0016-7037(80)90209-4.

Humphris, S. E., G. Thompson, J.-G. Schilling, and R. H. Kingsley (1985), Petrological and geochemical variations along the Mid-Atlantic Ridge between 46°S and 32°S: Influence of the Tristan da Cunha mantle plume, *Geochim. Cosmochim. Acta*, *49*(6), 1445–1464, doi:10.1016/0016-7037(85)90294-7.

Ito, E., W. M. White, V. Von Drach, A. W. Hofmann, and D. E. James (1980), Isotopic studies of ocean ridge basalts, *Carnegie Institution Department of Terrestrial Magnetism Annual Report to the Director*, 465–471.

Jambon, A., B. Déruelle, G. Dreibus, and F. Pineau (1995), Chlorine and bromine abundance in MORB: the contrasting behaviour of the Mid-Atlantic Ridge and East Pacific Rise and implications for chlorine geodynamic cycle, *Chem. Geol.*, *126*(2), 101–117, doi:10.1016/0009-2541(95)00112-4.

Jenner, F. E., and H. S. C. O'Neill (2012a), Major and trace analysis of basaltic glasses by laser-ablation ICP-MS, *Geochem. Geophys. Geosyst.*, *13*, doi:10.1029/2011gc003890.

Jenner, F. E., and H. S. C. O'Neill (2012b), Analysis of 60 elements in 616 ocean floor basaltic glasses, *Geochem. Geophys. Geosyst.*, *13*, doi:10.1029/2011gc004009.

Jochum, K. P., and S. P. Verma (1996), Extreme enrichment of Sb, Tl and other trace elements in altered MORB, *Chem. Geol.*, *130*, 289-299.

Jochum, K. P., and A. W. Hofmann (1997), Constraints on earth evolution from antimony in mantle-derived rocks, *Chem. Geol.*, *139*(1–4), 39–49, doi:10.1016/s0009-2541(97)00032-6.

Jochum, K. P., A. W. Hofmann, and H. M. Seufert (1993), Tin in mantle-derived rocks: Constraints on Earth

evolution, *Geochim. Cosmochim. Acta*, *57*(15), 3585–3595, doi:10.1016/0016-7037(93)90141-i.

Joron, J. L. (1980), Géochimie des éléments en traces du volcanisme de l'Afar et de la mégastructure Mer Rouge-Afar-Golfe d'Aden. Implications pétrogénétiques et géodynamiques, *Bulletin de la Société géologique de France*, *22*, 945.

Kingsley, R. H. (2002), The geochemistry of basalts from the Easter microplate boundaries and the western Easter-Salas y Gomez seamount chain: A comprehensive study of mantle plume-spreading center interaction, *Doctoral Dissertation, University of Rhode Island*.

Kingsley, R. H., and J.-G. Schilling (1995), Carbon in Mid-Atlantic Ridge basalt glasses from 28°N to 63°N: Evidence for a carbon-enriched Azores mantle plume, *Earth Planet Sci. Lett.*, *129*(1–4), 31–53, doi:10.1016/0012-821x(94)00241-p.

Kingsley, R. H., and J.-G. Schilling (1998), Plume-ridge interaction in the Easter-Salas y Gomez seamount chain-Easter Microplate system: Pb isotope evidence, *J. Geophys. Res.*, *103*(B10), 24159–24177, doi:10.1029/98jb01496.

Kingsley, R. H., J. Blichert-Toft, D. Fontignie, and J.-G. Schilling (2007), Hafnium, neodymium, and strontium isotope and parent-daughter element systematics in basalts from the plume-ridge interaction system of the Salas y Gomez Seamount Chain and Easter Microplate, *Geochem. Geophys. Geosyst.*, *8*(4), Q04005, doi:10.1029/2006gc001401.

Kingsley, R. H., J.-G. Schilling, J. E. Dixon, P. Swart, R. Poreda, and K. Simons (2002), D/H ratios in basalt glasses from the Salas y Gomez mantle plume interacting with the East Pacific Rise: Water from old D-rich recycled crust or primordial water from the lower mantle?, *Geochem. Geophys. Geosyst.*, *3*(4), 1025, doi:10.1029/2001gc000199.

Klein, E. M., and C. H. Langmuir (1987), Global correlations of ocean ridge basalt chemistry with axial depth and crustal thickness, *J. Geophys. Res.*, *92*(B8), 8089–8115.

Kurz, M. D. (1982), Helium isotope geochemistry of oceanic volcanic rocks: Implications for mantle heterogeneity and degassing, *WHOI Technical Reports*, *82*.

Kurz, M. D., A. P. le Roex, and H. J. B. Dick (1998), Isotope Geochemistry of the Oceanic Mantle Near the Bouvet Triple Junction, *Geochim. Cosmochim. Acta*, *62*(5), 841–852, doi:10.1016/s0016-7037(97)00383-9.

Kyser, T. K., and J. R. O'Neil (1984), Hydrogen isotope systematics of submarine basalts, *Geochim. Cosmochim. Acta*, *48*(10), 2123–2133, doi:10.1016/0016-7037(84)90392-2.

le Roex, A. P. (1998), PetDB Submitted Data Set: Major and trace element and mineral compositions of basalts from the Agulhas 32 cruise, Southern Mid-Atlantic ridge.

le Roex, A. P., H. J. B. Dick, L. Gulen, A. M. Reid, and A. J. Erlank (1987), Local and regional heterogeneity in MORB from the Mid-Atlantic Ridge between 54.5°S and 51°S: Evidence for geochemical enrichment, *Geochim. Cosmochim. Acta*, *51*(3), 541–555, doi:10.1016/0016-7037(87)90068-8.

Le Roux, P. J. (2000), The geochemistry of selected mid-ocean ridge basalts from the southern Mid-Atlantic ridge (40-55°S), *Doctoral Dissertation, University of Cape Town*.

le Roux, P. J., A. P. le Roex, J. G. Schilling, N. Shimizu, W. W. Perkins, and N. J. G. Pearce (2002a), Mantle heterogeneity beneath the southern Mid-Atlantic Ridge: trace element evidence for contamination of ambient asthenospheric mantle, *Earth Planet Sci. Lett.*, *203*(1), 479–498, doi:10.1016/s0012-821x(02)00832-4.

le Roux, P. l. R., A. l. R. le Roex, and J. G. S. Schilling (2002b), Crystallization processes beneath the southern Mid-Atlantic Ridge (40-55°S), evidence for high-pressure initiation of crystallization, *Contrib. Mineral. Petrol.*, *142*(5), 582–602, doi:10.1007/s00410-001-0312-y.

Lehnert, K., Y. Su, C. H. Langmuir, B. Sarbas, and U. Nohl (2000), A global geochemical database structure for rocks, *Geochem. Geophys. Geosyst.*, *1*(5), 1-14, doi:10.1029/1999gc000026.

Macdougall, J. D., and G. W. Lugmair (1986), Sr and Nd isotopes in basalts from the East Pacific Rise: significance for mantle heterogeneity, *Earth Planet Sci. Lett.*, *77*(3–4), 273–284, doi:10.1016/0012-821x(86)90139-1.

Marty, B., and M. Ozima (1986), Noble gas distribution in oceanic basalt glasses, *Geochim. Cosmochim. Acta*, *50*(6), 1093–1097, doi:10.1016/0016-7037(86)90390-x.

Marty, B., and A. Jambon (1987), C^3He in volatile fluxes from the solid Earth: implications for carbon geodynamics, *Earth Planet Sci. Lett.*, *83*(1–4), 16–26, doi:10.1016/0012-821x(87)90047-1.

Melson, W. G., T. O'Hearn, and E. Jarosewich (2002), A data brief on the Smithsonian Abyssal Volcanic Glass Data File, *Geochem. Geophys. Geosyst.*, *3*(4), doi:10.1029/2001GC000249.

Michael, P. (1988), The concentration, behavior and storage of H_2O in the suboceanic upper mantle: Implications for mantle metasomatism, *Geochim. Cosmochim. Acta*, *52*, 555–566.

Michael, P. (1995), Regionally distinctive sources of depleted MORB: Evidence from trace elements and H_2O, *Earth Planet Sci. Lett.*, *131*(3–4), 301–320, doi:10.1016/0012-821X(95)00023-6.

Michael, P. J., and W. C. Cornell (1998), Influence of spreading rate and magam supply on crystallization and assimilation beneath mid-ocean ridges: Evidence from chlorine and major element chemistry of mid-ocean ridge basalts, *J. Geophys. Res.*, *103*, 18325–18356.

Moore, J., and J. Schilling (1973), Vesicles, water, and sulfur in Reykjanes Ridge basalts, *Contrib. Mineral. Petrol.*, *41*(2), 105–118, doi:10.1007/bf00375036.

Moreira, M., T. Staudacher, P. Sarda, J.-G. Schilling, and C. J. Allègre (1995), A primitive plume neon component in MORB: The Shona ridge-anomaly, South Atlantic (51°S), *Earth Planet Sci. Lett.*, *133*(3–4), 367–377, doi:10.1016/0012-821x(95)00080-v.

Muehlenbachs, K., and R. N. Clayton (1972), Oxygen Isotope Studies of Fresh and Weathered Submarine Basalts, *Can. J. Earth Sci.*, *9*(2), 172–184, doi:10.1139/e72-014.

Nakamura, N. (1974), Determination of REE, Ba, Fe, Mg, Na and K in carbonaceous and ordinary chondrites, *Geochim. Cosmochim. Acta*, *38*, 757–775.

Neumann, E.-R., and J.-G. Schilling (1984), Petrology of basalts from the Mohns-Knipovich Ridge; the Norwegian-Greenland Sea, *Contrib. Mineral. Petrol.*, *85*(3), 209–223, doi:10.1007/bf00378101.

Pan, Y., and R. Batiza (1998), Major element chemistry of volcanic glasses from the Easter Seamount Chain: Constraints on melting conditions in the plume channel, *J. Geophys. Res.*, *103*(B3), 5287–5304, doi:10.1029/97jb03617.

Patchett, P. J., and M. Tatsumoto (1980), Hafnium isotope variations in oceanic basalts, *Geophys. Res. Lett.*, *7*(12), 1077–1080, doi:10.1029/GL007i012p01077.

Pineau, F., and M. Javoy (1994), Strong degassing at ridge crests: The behaviour of dissolved carbon and water in basalt glasses at 14°N, Mid-Atlantic Ridge, *Earth Planet Sci. Lett.*, *123*(1–3), 179–198, doi:10.1016/0012-821x(94)90266-6.

Poreda, R., and F. R. d. Brozolo (1984), Neon isotope variations in Mid-Atlantic Ridge basalts, *Earth Planet Sci. Lett.*, *69*(2), 277–289, doi:10.1016/0012-821x(84)90187-0.

Poreda, R., J. G. Schilling, and H. Craig (1986), Helium and hydrogen isotopes in ocean-ridge basalts north and south of

Iceland, *Earth Planet Sci. Lett.*, *78*(1), 1–17, doi:10.1016/0012-821x(86)90168-8.

Poreda, R. J., J. G. Schilling, and H. Craig (1993), Helium isotope ratios in Easter microplate basalts, *Earth Planet Sci. Lett.*, *119*(3), 319–329, doi:10.1016/0012-821x(93)90141-u.

Righter, K. (2003), Metal-Silicate partitioning of siderophile elements and core formation in the early Earth, *Annu. Rev. Earth Planet. Sci.*, *31*(1), 135–174, doi:10.1146/annurev.earth.31.100901.145451.

Rooney, T. O., B. B. Hanan, D. W. Graham, T. Furman, J. Blichert-Toft, and J. G. Schilling (2012), Upper Mantle Pollution during Afar Plume-Continental Rift Interaction, *J. Petrol.*, *53*(2), 365–389, doi:10.1093/petrology/egr065.

Rowe, E. C., and J. G. Schilling (1979), Fluorine in Iceland and Reykjanes Ridge basalts, *Nature*, *279*(5708), 33–37.

Rubin, K. H., and J. D. Macdougall (1988), ^{226}Ra excesses in mid-ocean-ridge basalts and mantle melting, *Nature*, *335*(6186), 158–161.

Rubin, K. H., and J. D. Macdougall (1990), Dating of neovolcanic MORB using (^{226}Ra/^{230}Th) disequilibrium, *Earth Planet Sci. Lett.*, *101*(2–4), 313–322, doi:10.1016/0012-821x(90)90162-q.

Ryan, J. G., and C. H. Langmuir (1987), The systematics of lithium abundances in young volcanic rocks, *Geochim. Cosmochim. Acta*, *51*(6), 1727–1741, doi:10.1016/0016-7037(87)90351-6.

Ryan, W. B. F., et al. (2009), Global Multi-Resolution Topography synthesis, *Geochem. Geophys. Geosyst.*, *10*(3), doi:10.1029/2008gc002332.

Sarda, P., T. Staudacher, and C. J. Allègre (1988), Neon isotopes in submarine basalts, *Earth Planet Sci. Lett.*, *91*(1-2), 73–88, doi:10.1016/0012-821x(88)90152-5.

Sarda, P., M. Moreira, T. Staudacher, J.-G. Schilling, and C. J. Allègre (2000), Rare gas systematics on the southernmost Mid-Atlantic Ridge: Constraints on the lower mantle and the Dupal source, *J. Geophys. Res.*, *105*(B3), 5973–5996, doi:10.1029/1999jb900282.

Schiano, P., J.-L. Birck, and C. J. Allègre (1997), Osmium-strontium-neodymium-lead isotopic covariations in mid-ocean ridge basalt glasses and the heterogeneity of the upper mantle, *Earth Planet Sci. Lett.*, *150*(3–4), 363–379, doi:10.1016/s0012-821x(97)00098-8.

Schilling, J.-G., R. H. Kingsley, B. B. Hanan, and B. L. McCully (1992), Nd-Sr-Pb Isotopic Variations Along the Gulf of Aden: Evidence for Afar Mantle Plume-Continental Lithosphere Interaction, *J. Geophys. Res.*, *97*(B7), 10927–10966, doi:10.1029/92jb00415.

Schilling, J.-G., D. Fontignie, J. Blichert-Toft, R. Kingsley, and U. Tomza (2003), Pb-Hf-Nd-Sr isotope variations along the Galápagos Spreading Center (101°-83°W): Constraints on the dispersal of the Galápagos mantle plume, *Geochem. Geophys. Geosyst.*, *4*(10), 8512, doi:10.1029/2002gc000495.

Schilling, J. G. (1973), Iceland Mantle Plume: Geochemical Study of Reykjanes Ridge, *Nature*, *242*(5400), 565–571.

Schilling, J. G. (1975), Azores mantle blob: Rare-earth evidence, *Earth Planet Sci. Lett.*, *25*(2), 103–115, doi:10.1016/0012-821x(75)90186-7.

Schilling, J. G., R. N. Anderson, and P. Vogt (1976), Rare earth, Fe and Ti variations along the Galapagos spreading centre, and their relationship to the Galapagos mantle plume, *Nature*, *261*(5556), 108–113.

Schilling, J. G., R. H. Kingsley, and J. D. Devine (1982), Galápagos Hot Spot-Spreading Center System 1. Spatial Petrological and Geochemical Variations (83°W-101°W), *J. Geophys. Res.*, *87*(B7), 5593–5610, doi:10.1029/JB087iB07p05593.

Schilling, J. G., M. B. Bergeron, R. Evans, and J. V. Smith (1980), Halogens in the Mantle Beneath the North Atlantic [and Discussion], *Phil. Trans. Roy. Soc. Lond. Math. Phys. Sci.*, *297*(1431), 147–178.

Schilling, J. G., H. Sigurdsson, A. N. Davis, and R. N. Hey (1985), Easter microplate evolution, *Nature*, *317*(6035), 325–331.

Schilling, J. G., B. B. Hanan, B. McCully, R. H. Kingsley, and D. Fontignie (1994), Influence of the Sierra Leone mantle plume on the equatorial Mid-Atlantic Ridge: A Nd-Sr-Pb isotopic study, *J. Geophys. Res.*, *99*(B6), 12005–12028, doi:10.1029/94jb00337.

Schilling, J. G., R. Kingsley, D. Fontignie, R. Poreda, and S. Xue (1999), Dispersion of the Jan Mayen and Iceland mantle plumes in the Arctic: A He-Pb-Nd-Sr isotope tracer study of basalts from the Kolbeinsey, Mohns, and Knipovich Ridges, *J. Geophys. Res.*, *104*(B5), 10543–10569, doi:10.1029/1999jb900057.

Schilling, J. G., M. Zajac, R. Evans, T. Johnston, W. White, J. D. Devine, and R. Kingsley (1983), Petrologic and geochemical variations along the Mid-Atlantic Ridge from 29°N to 73°N, *Am. J. Sci.*, *283*(6), 510–586, doi:10.2475/ajs.283.6.510.

Schilling, J. G., C. Ruppel, A. N. Davis, B. McCuIiy, S. A. Tighe, R. H. Kingsley, and J. Lin (1995), Thermal structure of the mantle beneath the equatorial Mid-Atlantic Ridge: Inferences from the spatial variation of dredged basalt glass compositions, *J. Geophys. Res.*, *100*(B6), 10057–10076, doi:10.1029/95jb00668.

Schneider, W., and H. Wachendorf (1973), Vulkanismus und Graben-Bildung im Roten Meer, *Geologische Rundschau*, *62*(3), 754–773, doi:10.1007/bf01820959.

Shibata, T., G. Thompson, and F. Frey (1979), Tholeiitic and alkali basalts from the Mid-Atlantic Ridge at 43°N, *Contrib. Mineral. Petrol.*, *70*(2), 127–141, doi:10.1007/bf00374441.

Sigurdsson, H. (1981), First-Order Major Element Variation in Basalt Glasses From the Mid-Atlantic Ridge: 29°N to 73°N, *J. Geophys. Res.*, *86*(B10), 9483–9502, doi:10.1029/JB086iB10p09483.

Sigurdsson, H., and J. G. Schilling (1976), Spinels in Mid-Atlantic Ridge basalts: Chemistry and occurrence, *Earth Planet Sci. Lett.*, *29*(1), 7–20, doi:10.1016/0012-821x(76)90021-2.

Simons, K., J. E. Dixon, J.-G. Schilling, R. H. Kingsley, and R. Poreda (2002), Volatiles in basaltic glasses from the Easter-Salas y Gomez Seamount Chain and Easter Microplate: Implications for geochemical cycling of volatile elements, *Geochem. Geophys. Geosyst.*, *3*(7), doi:10.1029/2001GC000173.

Sims, K. W. W., H. E. Newsom, and E. S. Gladney (1990), Chemical fractionation during formation of the Earth's core and continental crust: clues from As, Sb, W, and Mo, in Origin of Earth, edited by H. E. Newsom and J. H. Jones, pp. 291–317, Oxford Press.

Sinton, J. M., R. S. Detrick, J. P. Canales, G. Ito, and M. D. Behn (2003), Morphology and segmentation of the western Galápagos Spreading Center, 90.5°-98°W, *Geochem. Geophys. Geosys.*, *4*(12), doi:10.1029/2003GC000609.

Staudacher, T., P. Sarda, S. H. Richardson, C. J. Allègre, I. Sagna, and L. V. Dmitriev (1989), Noble gases in basalt glasses from a Mid-Atlantic Ridge topographic high at 14°N: geodynamic consequences, *Earth Planet Sci. Lett.*, *96*(1–2), 119–133, doi:10.1016/0012-821x(89)90127-1.

Sun, S.-S., and W. F. McDonough (1989), Chemical and isotopic systematics of oceanic basalts: implications for mantle composition and process, in Magmatism in the Ocean Basins, edited by A. D. Saunders and M. J. Norry, pp. 313–345.

Sun, S.-S., M. Tatsumoto, and J.-G. Schilling (1975), Mantle Plume Mixing Along the Reykjanes Ridge Axis: Lead Isotopic Evidence, *Science*, *190*(4210), 143–147.

Sun, W. (2003), Rhenium systematics in submarine MORB and back-arc basin glasses: laser ablation ICP-MS results, *Chem. Geol.*, *196*(1–4), 259–281, doi:10.1016/s0009-2541(02)00416-3.

Unni, C. K. (1976), Chlorine and bromine degassing during submarine and subaerial volcanism, *Doctoral Dissertation, University of Rhode Island*.

Unni, C. K., and J. G. Schilling (1978), Cl and Br degassing by volcanism along the Reykjanes Ridge and Iceland, *Nature*, *272*(5648), 19–23.

van Heerden, L. A., and A. P. Roex (1988), Petrogenesis of picrite and associated basalts from the southern Mid-Atlantic Ridge, *Contrib. Mineral. Petrol.*, *100*(1), 47–60, doi:10.1007/bf00399439.

Verma, S. P., and J.-G. Schilling (1982), Galapagos Hot Spot-Spreading Center System 2. $^{87}Sr/^{86}Sr$ And Large Ion Lithophile Element Variations (85°W-101°W), *J. Geophys. Res.*, *87*(B13), 10838–10856, doi:10.1029/JB087iB13p10838.

Verma, S. P., J. G. Schilling, and D. G. Waggoner (1983), Neodymium isotopic evidence for Galapagos hotspot-spreading centre system evolution, *Nature*, *306*(5944), 654–657.

Waggoner, D. G. (1989), An isotopic and trace element study of mantle heterogeneity beneath the Norwegian-Greenland Sea, *Doctoral Dissertation, University of Rhode Island*.

Walter, M. J., and Y. Thibault (1995), Partitioning of Tungsten and Molybdenum between Metallic Liquid and Silicate Melt, *Science*, *270*(5239), 1186–1189, doi:10.2307/2889220.

White, W. M. (1979), Geochemistry of basalts from the FAMOUS area: a reexamination, *Carnegie Institution Department of Terrestrial Magnetism Yearbook*.

White, W. M. (1993), $^{238}U/^{204}Pb$ in MORB and open system evolution of the depleted mantle, *Earth Planet Sci. Lett.*, *115*(1–4), 211–226, doi:10.1016/0012-821x(93)90223-v.

White, W. M., and W. B. Bryan (1977), Sr-isotope, K, Rb, Cs, Sr, Ba, and rare-earth geochemistry of basalts from the FAMOUS area, *Geol. Soc.Am. Bull.*, *88*(4), 571–576.

White, W. M., and J.-G. Schilling (1978), The nature and origin of geochemical variation in Mid-Atlantic Ridge basalts from the Central North Atlantic, *Geochim. Cosmochim. Acta*, *42*(10), 1501–1516, doi:10.1016/0016-7037(78)90021-2.

White, W. M., and A. W. Hofmann (1982), Sr and Nd isotope geochemistry of oceanic basalts and mantle evolution, *Nature*, *296*(5860), 821–825.

White, W. M., A. W. Hofmann, and H. Puchelt (1987), Isotope Geochemistry of Pacific Mid-Ocean Ridge Basalt, *J. Geophys. Res.*, *92*(B6), 4881-4893, doi:10.1029/JB092iB06p04881.

Wood, B., S. Nielsen, M. Rehkamper, and A. Halliday (2008), The effects of core formation on the Pb- and Tl- isotopic composition of the silicate Earth, *Earth Planet Sci. Lett.*, *269*(3–4), 326–336, doi:10.1016/j.epsl.2008.01.027.

Yi, W., A. N. Halliday, J. C. Alt, D.-C. Lee, M. Rehkämper, M. O. Garcia, C. H. Langmuir, and Y. Su (2000), Cadmium, indium, tin, tellurium, and sulfur in oceanic basalts: Implications for chalcophile element fractionation in the Earth, *J. Geophys. Res.*, *105*(B8), 18927–18948, doi:10.1029/2000jb900152.

Yu, D., D. Fontignie, and J.-G. Schilling (1997), Mantle plume-ridge interactions in the Central North Atlantic: A Nd isotope study of Mid-Atlantic Ridge basalts from 30°N to 50°N, *Earth Planet Sci. Lett.*, *146*(1-2), 259–272, doi:10.1016/s0012-821x(96)00221-x.